NASA/TM—2005–214061

Thermal Catalytic Oxidation of Airborne Contaminants by a Reactor Using Ultra-Short Channel Length, Monolithic Catalyst Substrates

(MSFC Center Director's Discretionary Fund Final Report, Project No. 02–18)

J.L. Perry and K.M.Tomes
Marshall Space Flight Center, Marshall Space Flight Center, Alabama

J.D. Tatara
Qualis Corporation, Huntsville, Alabama

September 2005

The NASA STI Program Office…in Profile

Since its founding, NASA has been dedicated to the advancement of aeronautics and space science. The NASA Scientific and Technical Information (STI) Program Office plays a key part in helping NASA maintain this important role.

The NASA STI Program Office is operated by Langley Research Center, the lead center for NASA's scientific and technical information. The NASA STI Program Office provides access to the NASA STI Database, the largest collection of aeronautical and space science STI in the world. The Program Office is also NASA's institutional mechanism for disseminating the results of its research and development activities. These results are published by NASA in the NASA STI Report Series, which includes the following report types:

- TECHNICAL PUBLICATION. Reports of completed research or a major significant phase of research that present the results of NASA programs and include extensive data or theoretical analysis. Includes compilations of significant scientific and technical data and information deemed to be of continuing reference value. NASA's counterpart of peer-reviewed formal professional papers but has less stringent limitations on manuscript length and extent of graphic presentations.

- TECHNICAL MEMORANDUM. Scientific and technical findings that are preliminary or of specialized interest, e.g., quick release reports, working papers, and bibliographies that contain minimal annotation. Does not contain extensive analysis.

- CONTRACTOR REPORT. Scientific and technical findings by NASA-sponsored contractors and grantees.

- CONFERENCE PUBLICATION. Collected papers from scientific and technical conferences, symposia, seminars, or other meetings sponsored or cosponsored by NASA.

- SPECIAL PUBLICATION. Scientific, technical, or historical information from NASA programs, projects, and mission, often concerned with subjects having substantial public interest.

- TECHNICAL TRANSLATION. English-language translations of foreign scientific and technical material pertinent to NASA's mission.

Specialized services that complement the STI Program Office's diverse offerings include creating custom thesauri, building customized databases, organizing and publishing research results…even providing videos.

For more information about the NASA STI Program Office, see the following:

- Access the NASA STI Program Home Page at ***http://www.sti.nasa.gov***

- E-mail your question via the Internet to help@sti.nasa.gov

- Fax your question to the NASA Access Help Desk at 301–621–0134

- Telephone the NASA Access Help Desk at 301–621–0390

- Write to:
  NASA Access Help Desk
  NASA Center for AeroSpace Information
  7121 Standard Drive
  Hanover, MD 21076–1320
  301–621–0390

NASA/TM—2005–214061

Thermal Catalytic Oxidation of Airborne Contaminants by a Reactor Using Ultra-Short Channel Length, Monolithic Catalyst Substrates

(MSFC Center Director's Discretionary Fund Final Report, Project No. 02–18)

J.L. Perry and K.M.Tomes
Marshall Space Flight Center, Marshall Space Flight Center, Alabama

J.D. Tatara
Qualis Corporation, Huntsville, Alabama

National Aeronautics and
Space Administration

Marshall Space Flight Center • MSFC, Alabama 35812

September 2005

TRADEMARKS

Available from:

NASA Center for AeroSpace Information
7121 Standard Drive
Hanover, MD 21076–1320
301–621–0390

National Technical Information Service
5285 Port Royal Road
Springfield, VA 22161
703–487–4650

TABLE OF CONTENTS

TABLE OF CONTENTS (Continued)

LIST OF FIGURES

LIST OF FIGURES (Continued)

LIST OF TABLES

LIST OF ACRONYMS AND SYMBOLS

Al_2O_3	alumina
ASHRAE	American Society of Heating, Refrigerating, and Air Conditioning Engineers
BMP	micro-impurity adsorption system (Russian acronym)
C_3F_8	octafluoropropane
CH_4	methane
CO	carbon monoxide
CO_2	carbon dioxide
ECLSS	Environmental Control and Life Support System
FAA	Federal Aviation Administration
GHSV	gas hourly space velocity
GRC	Glenn Research Center
H_2	hydrogen
H_2O	water
H_3PO_4	phosphoric acid
HCHO	formaldehyde
HTCO	high-temperature catalytic oxidation
ISS	*International Space Station*
LiOH	lithium hydroxide
NH_3	ammonia
PACRATS	Payloads and Real-time Automated Test System

LIST OF ACRONYMS AND SYMBOLS (Continued)

PCI	Precision Combustion, Inc.
Pd	palladium
PKF-T	thermal catalytic oxidation module (Russian acronym)
PMMS	Process Material Management System
RLSE	regenerative life support equipment
SF_6	sulfur hexafluoride
SMAC	spacecraft maximum allowable concentration
TCC	trace contaminant control
TCCS	trace contaminant control subassembly
TCO	thermal catalytic oxidizer
THC	temperature and humidity control
UPS	uninterruptable power supply
USCM	ultra-short channel length, monolithic
VOC	volatile organic compound

TECHNICAL MEMORANDUM

THERMAL CATALYTIC OXIDATION OF AIRBORNE CONTAMINANTS BY A REACTOR USING ULTRA-SHORT CHANNEL LENGTH, MONOLITHIC CATALYST SUBSTRATES

(MSFC Center Director's Discretionary Fund Final Report, Project No. 02–18)

1. BACKGROUND

Contaminated air and process gases—whether in a crewed spacecraft cabin atmosphere, the working volume of a microgravity science or ground-based laboratory experiment facility, or the exhaust from an automobile—are pervasive problems that ultimately affect human health, performance, and well being. The need for highly effective, economical decontamination processes spans a wide range of terrestrial and space flight applications. Typically, gas decontamination relies upon adsorption and absorption processes. For economic reasons, most industrial packed-bed adsorption processes use activated carbon. It is cheap and highly effective for most applications. Once saturated, the adsorbent is a concentrated source of contaminants. For industrial applications, the carbon is either dumped or regenerated. Regeneration may be accomplished in situ or at an offsite location. In either case, the dumped carbon and concentrated waste streams resulting from regeneration constitute a hazard that must be handled appropriately to minimize environmental impact. As economic and regulatory forces drive toward minimizing waste streams and environmental impact, thermal catalytic oxidation is moving to the forefront of cleaner gas decontamination processes. By tailoring the reactor and catalyst design, more complete contaminant destruction is achieved, leading to reduced waste handling, process downtime, and maintenance.

As with industrial applications, spacecraft life support systems and payload facilities rely heavily on adsorption, particularly via activated carbon, to remove contaminants. Regeneration is most frequently accomplished by replacing the saturated adsorbent with fresh media. Some processes employ in situ thermal-vacuum swing regeneration. While adsorption can remove most volatile contaminants from air and process gas streams, light hydrocarbons and alcohols along with carbon monoxide (CO) are best removed using thermal catalytic oxidation. Therefore, thermal catalytic oxidation is a key unit operation within any broad spectrum air or gas decontamination process. For thermal catalytic oxidation to be viable, however, it must be proven to be safe, reliable, and consume minimal power.

Trade assessments of candidate thermal catalytic oxidation process technologies have demonstrated that a unique reactor design based upon an ultra-short channel length, monolithic (USCM) substrate provides the solution for improving process economics and performance of thermal catalytic oxidation processes over traditional reactor designs employing catalysts supported on pellets or ceramic monoliths. The versatility of the USCM substrate may expand the use of thermal catalytic oxidation to a wider range of space flight and terrestrial applications as well as boost performance by increasing process capacity. The USCM substrate, developed by Precision Combustion, Inc. (PCI), North Haven, CT, and adapted to space flight applications under NASA guidance, uses a series of short channel length, high cell density monoliths to provide a high catalytic conversion efficiency while minimizing boundary layer buildup and reactor size.

Potential space flight applications include cabin air quality control and payload process gas purification. Both applications are dominated by adsorption processes that rely on expendable resources. While adsorption is a proven process for cleaning process gases, the expendable materials used possess high operating costs primarily associated with ground-based equipment processing and Earth-to-orbit transportation. Eliminating or reducing the reliance on adsorption in these applications will lead to improved process economics and operational flexibility.

In order to fully understand the benefits of a USCM substrate, it is necessary to integrate it with a highly efficient recuperative heat exchanger and operate the integrated assembly under a range of electrical power and process airflow conditions that bound the potential range of space flight applications. To this end, performance of a prototype USCM-based reactor has been characterized under a variety of process flow and contaminant loading conditions. The observed performance is evaluated against that of gas purification processes presently used on board NASA’s crewed spacecraft.

2. PROJECT SUMMARY

A prototype thermal catalytic reactor based on the USCM substrate was integrated into a test stand that provided varying process gas flow, electrical power input, and contaminant loading conditions. The experiment was based upon a fractional factorial design that allows robust design techniques to be used for future process scale-up. Data were collected on electrical power input, thermal transient duration, and pressure drop at varying process flow conditions. Chemical contaminants representative of the various niche applications for the USCM technology were injected into the process gas stream. Contaminant oxidation efficiency was monitored. An endurance test was conducted to determine reactor life and maintenance schedules. Results are used to compare the performance and process economics of the USCM-based system to existing technologies in use by NASA for process gas and cabin air decontamination on board the *International Space Station* (*ISS*). As well, the results may serve as a design basis for future applications in process gas purification and cabin air quality control for NASA's spacecraft and space habitats contained in the vision for space exploration.

3. PURPOSE AND OBJECTIVES

The purpose of this project is to demonstrate the integration of a USCM-based thermal catalytic reactor with a recuperative heat exchanger and characterize its performance under varying process conditions, namely, process airflow and electrical power input.

Primary project objectives are the following:

- Evaluate destruction of a variety of contaminants under varying process flow conditions.
- Evaluate resource requirements under varying process flow conditions.
- Evaluate the USCM's process economics when incorporated in niche applications.
- Provide data necessary to serve as a basis for process scale-up.

Secondary objectives addressed as a matter of course during the project's conduct are the following:

- Demonstrate the physical integration of the USCM with an *ISS* trace contaminant control subassembly (TCCS) flight-like recuperative heat exchanger.
- Determine the duration of the thermal transient experienced by the integrated test article/heat exchanger assembly at varying process airflow rate conditions and electrical power inputs.
- Determine the lag between the time electrical power is applied to the test article and the time that oxidation reaction light-off occurs.
- Characterize the test article's steady state electrical power requirements under low, moderate, and high process airflow conditions.

4. TECHNOLOGY OVERVIEW

Descriptions of the USCM thermal catalytic reactor technology and potential niche applications are provided in sections 4.1 and 4.2.

4.1 Ultra-Short Channel Length, Monolithic Thermal Catalytic Reactor

The USCM thermal catalytic reactor technology developed by PCI is based on an innovative reactor design approach that uses a static mixer as the catalyst substrate. Coating catalysts on a static mixer has been the focus of several notable projects outside NASA; however, none of these efforts have specifically addressed nonindustrial applications. The USCM thermal catalytic reactor technology addresses the unique requirements of portable gas and process exhaust conditioning for the automotive industry. Many of these requirements apply to space transportation.

The USCM thermal catalytic oxidation reactor (fig. 1) is composed of structured substrate consisting of a series of high cell density, ultra-short channel length, metal monoliths. The catalyst is applied to the substrate via a specialized coating process that resists spalling. The reactor design will improve both process economics and performance since the series of USCMs provide a significant reduction in boundary layer buildup that occurs in conventional monolithic substrates. A comparison of the boundary layer buildup of the USCM-based reactor with that of a conventional ceramic monolith is illustrated in figure 2. Performance characteristics are compared to conventional monolithic and pellet substrates in table 1. As can be seen, the USCM technology provides significantly improved mass transfer performance. As well, thermal mass is reduced. This may lead to smaller, less power-intensive reactors for an expanded suite of space flight applications.[1–3]

4.2 Ultra-Short Channel Length, Monolithic Technology Applications

Application of the USCM thermal catalytic reactor technology ranges from spacecraft cabin air quality control to payload process gas purification. A brief description of principal applications is provided in sections 4.2.1 through 4.2.3.

4.2.1 Spacecraft Cabin Air Quality Control

Spacecraft cabin air quality control is provided by a variety of processes. A brief history and descriptions of the systems used for trace contaminant control during the course of the U.S. Space program are provided in reference 4. The typical processes rely upon physical or chemical adsorption and employ granular activated charcoal or zeolite as the adsorbent media. Chemical treatment of the adsorbent media is employed when necessary to enhance the removal of some contaminants, such as ammonia (NH_3) and formaldehyde (HCHO). Ambient temperature catalytic oxidation using a supported platinum group metal has been employed to remove CO from cabin atmospheres on board the Shuttle, Spacelab, *Mir*, and presently, the Russian segment of the *ISS*. Thermal catalytic oxidation was used for the first time on a spacecraft when the *ISS*'s U.S. Laboratory Module, Destiny, was activated in February 2001.

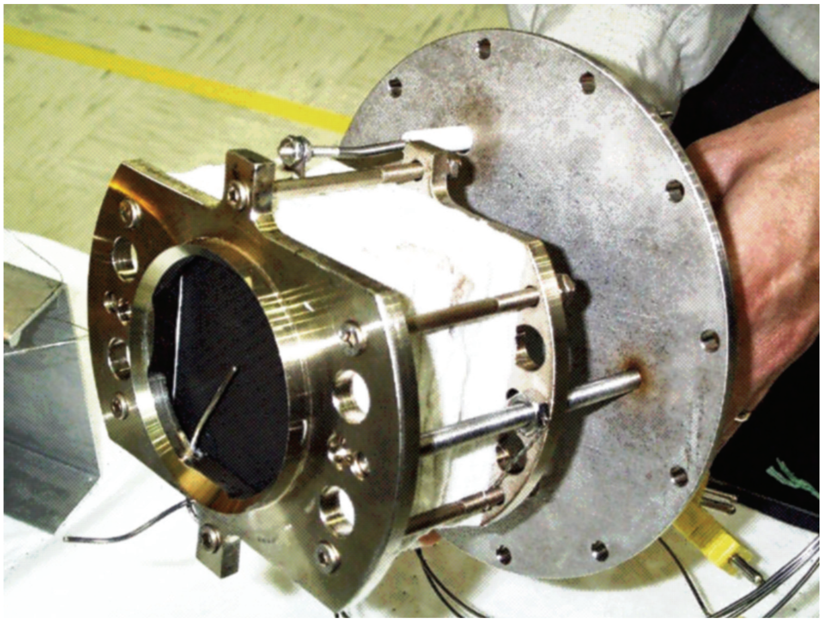

Figure 1. Prototype USCM reactor.

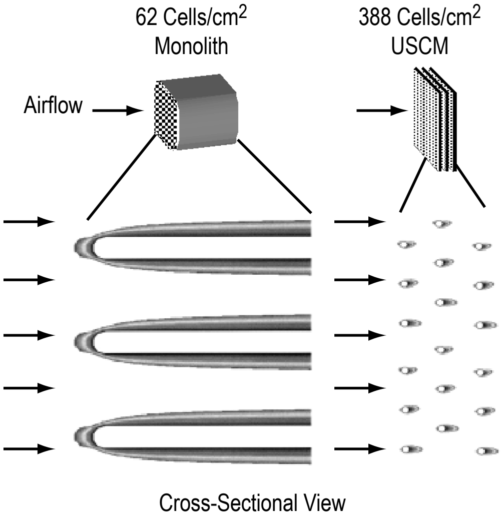

Figure 2. Comparison of boundary layer buildup in monolithic substrates.

Table 1. Catalyst substrate physical properties.

Property	Substrate		
	USCM	Pellet	Monolith
Cell density (cpsc)	388	NA	62
Void fraction	0.62	0.4	0.65
Surface area (cm^2/cm^3)	62	11	19
Mass transfer coefficient (cm/s)*	68	19	6.7
Heat transfer coefficient (W/m^2K)*	640	120	51

* 350 °C air at 3.1 m/s; mass transfer based on propylene diffusion in air.

The TCCS included in Destiny's atmosphere revitalization subsystem (fig. 3) utilizes activated charcoal adsorption, thermal catalytic oxidation, and lithium hydroxide (LiOH) chemisorption to remove trace chemical contaminants and acidic oxidation products from the cabin atmosphere. Air enters the TCCS at 15.29 m^3/hr (9 ft^3/min) and flows through a fixed bed containing 22.7 kg (50 lb) of 4 × 6 mesh Barnebey-Sutcliffe Corp. type 3032 activated charcoal. This charcoal is treated with 10 wt.% phosphoric acid (H_3PO_4) to remove NH_3 via chemisorption. Key design drivers for the charcoal bed's size and flow are NH_3 and dichloromethane. After flowing through the fixed bed, 4.59 m^3/hr (2.7 ft^3/min) is diverted through a thermal catalytic oxidizer (TCO). Components of the TCO include a plate-fin recuperative heat exchanger, a heater assembly, and a catalyst bed. The catalyst bed is packed with 0.5 kg (1.1 lb) of 3.2-mm cylindrical alumina (Al_2O_3) pellets which support a 0.5-percent palladium (Pd) precious metal catalyst. The catalyst is manufactured by Engelhard Corp. Under normal process conditions, the temperature within the TCO is maintained at 400 °C (750 °F). An operating temperature of up to 538 °C (1,000 °F) can be achieved if needed. Key design compounds driving the TCO's size, flow rate, and operating conditions are methane (CH_4) and CO. The TCO is specifically targeted as a niche application for the USCM technology. The air exiting the TCO flows through a fixed bed containing 1.4 kg (3 lb) of 6 × 14 mesh granular anhydrous LiOH to remove any acidic oxidation products. The LiOH is manufactured by Cyprus Foote Mineral Co. Downstream of the fixed LiOH bed, the flow streams combine and then exit the TCCS.[5]

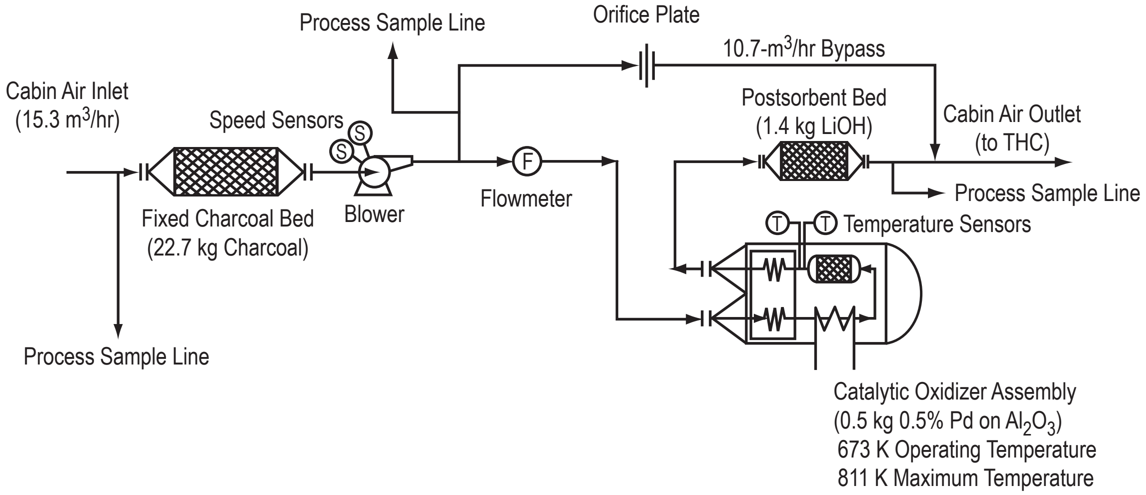

Figure 3. *ISS* TCCS process and instrumentation diagram.

The air quality control function on board the *ISS*'s Russian segment is provided by the micro-impurity adsorption system (Russian acronym BMP). This system employs activated charcoal adsorption and ambient temperature catalytic oxidation to remove trace contaminants and CO from the cabin atmosphere (fig. 4). In 2004 the BMP was retrofit with a thermal catalytic oxidation module known as the PKF-T. As shown in figure 4, 27 m^3/hr of cabin air first flows through a fixed bed of activated charcoal. This bed is expendable and contains 1.3 kg of charcoal. It is sized to remove compounds with molecular weights >80 g/mole that can foul the downstream regenerable charcoal beds. After exiting the expendable charcoal bed, the flow stream splits between two regenerable charcoal beds. Each of these beds contain 7.4 kg of charcoal. The beds are regenerated by a thermal and pressure swing process every 20 days. During this process, the beds are evacuated to space and heated to 200 °C. Downstream of the regenerable charcoal beds, the flow streams combine and flow through a bed containing 0.5 kg of platinum group metal catalyst. Carbon monoxide is converted to carbon dioxide (CO_2) in this bed.[6,7]

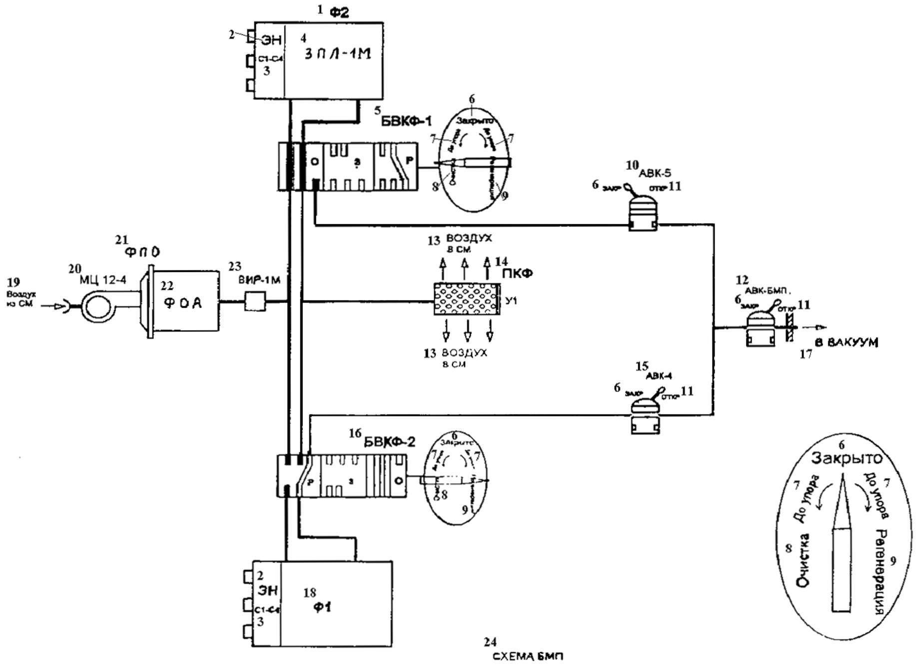

Figure 4. Russian segment BMP process and instrumentation diagram.

The PKF-T thermal catalytic oxidation unit was retrofit to the BMP during 2004. Figure 5 shows that 0.5 to 0.6 m^3/hr, or up to 2 percent, of the flow exiting the ambient temperature catalyst bed is diverted into the PKF-T. The normal operating temperature is 170 °C (338 °F). When required, the process temperature can be maintained between 250 °C (482 °F) and 270 °C (518 °F). In this temperature range, CH_4 oxidation efficiency is >50 percent. The exhaust from the PKF-T is returned to the BMP inlet to remove any harmful oxidation products.

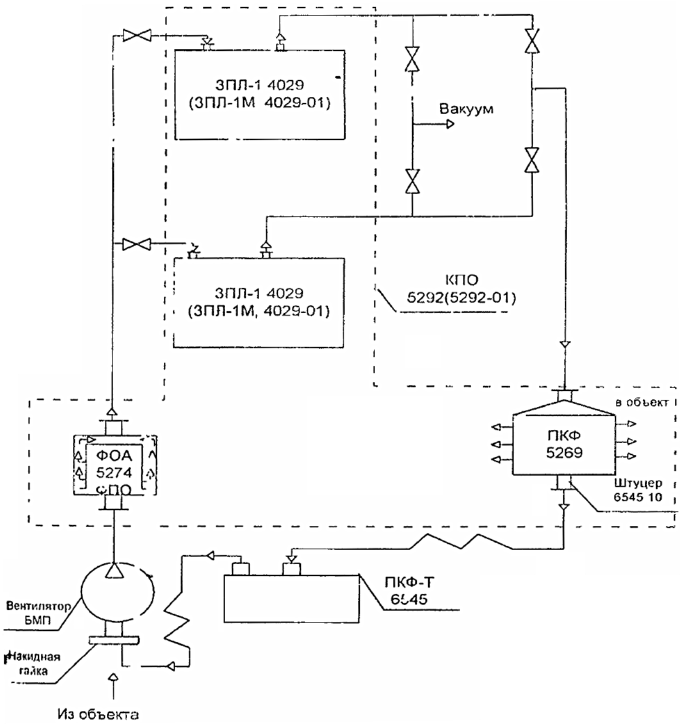

Figure 5. BMP showing PKF-T retrofit.

Future trace contaminant control system design is embracing the best features of the equipment presently used on board the *ISS* by combining regenerable adsorbents and thermal catalytic oxidation.[8] Simplifying the advanced design by using the expendable and regenerable adsorbent bed components from the BMP and the TCO from the TCCS addresses the significant logistics, maintenance, and performance deficiencies associated with the two individual systems. The result is a system providing broad spectrum trace contaminant control and possessing substantially lower logistics and maintenance requirements. Such a combination of TCC components was recommended by an early Space Station study report prepared by Battelle, Columbus, OH.[9] In such a system, the only area remaining for optimization is the method by which the thermal catalytic oxidation and adsorbent media are supported.

The USCM substrate is intended to replace the existing pellet-supported catalyst bed and heater assemblies in the TCO (fig. 6) and ultimately the granular adsorbent media to achieve a smaller size, more efficient operations, and ease of maintenance.[10] Because the USCM is modular, it is more amenable to on-orbit maintenance than the existing packed beds of catalyst and adsorbent media. Its low thermal mass allows for direct heating of the USCM substrate and, therefore, allows the reactor to reach operating temperature virtually instantaneous. This also applies to adsorbent beds where thermal swing regeneration is used. The application of the USCM substrate to present and future TCC system designs will allow for more flexible operations during both normal and contingency situations.

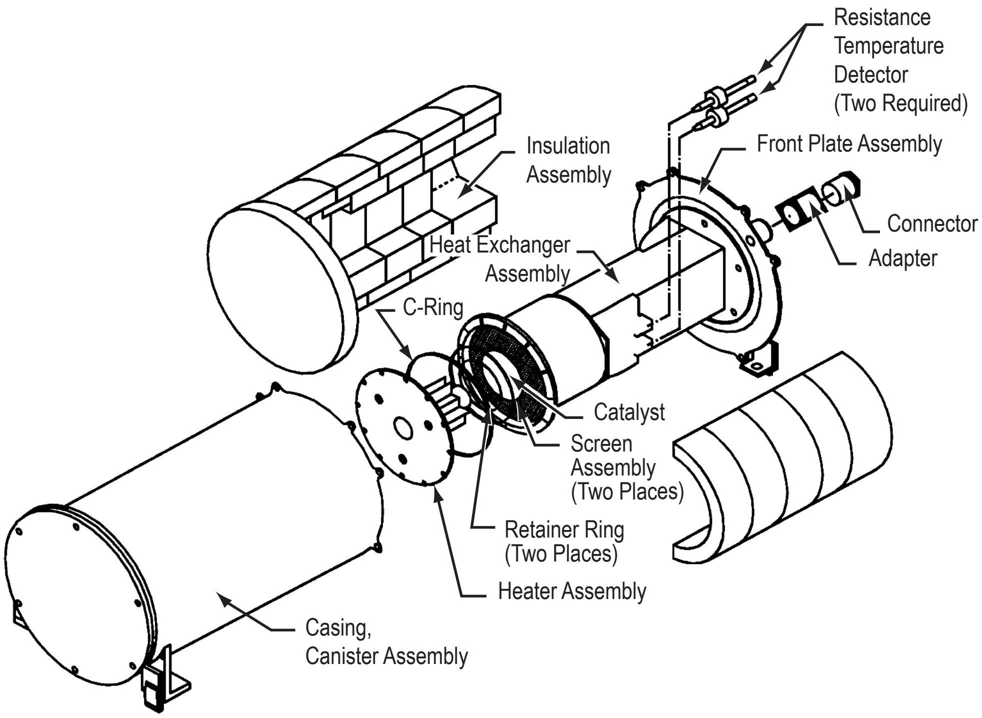

Figure 6. Trace contaminant control TCO for *ISS*.

4.2.2 Payload Process Gas Conditioning

During Space Station development, early concepts for handling a variety of payload process materials and wastes included both distributed and centralized systems. The overall laboratory module waste-handling system was known as the Process Material Management System (PMMS).[11] During the course of PMMS development, a variety of payload facilities was reviewed to bound the process design. From this review, it was found that most contamination that may be produced consists of volatile organic compounds (VOCs), particularly cleaning solvents such as alcohols and acetone.

As the Space Station design matured, it became apparent that the PMMS concept was highly complex and could lead to significant chemical handling safety and compatibility hazards over the life of the Station. The concept was scaled back to provide glovebox facilities on board the Station in which to conduct payload operations that require isolation from the cabin environment. Isolation is required for some payload operations either because the process is sensitive to the cabin environment or there is additional containment required to adequately protect the cabin environment from the process. Again, evaluation of proposed payload operations identified VOCs as the most significant contaminants that a glovebox process air purification unit would have to control. Low molecular weight alcohols, toluene, and ketones were among the chief design-driving compounds. Trade studies recommended a glovebox working volume contamination control ventilation approach of ventilation combined with thermal catalytic oxidation. Gas conditioning system performance included process airflow rates up to 3.4 m^3/hr and the ability to handle contaminant loadings as high as 10 times the spacecraft maximum allowable concentration (SMAC) at the inlet. Contaminant concentrations in the exhaust were to be below individual contaminant SMAC.

4.2.3 Indoor Air Quality

A recent review of space technologies and their terrestrial applications has stated that "indoor air quality is poised to top the list of global environmental issues for the twenty-first century."[12] In this light, it is not surprising to find striking similarity between air quality in a spacecraft cabin and terrestrial office buildings.[13] Technologies developed for spacecraft will be instrumental in addressing many of the commercial and residential problems associated with indoor air quality.[14] Studies have demonstrated that exposures to solvent-like VOCs in the range of 0.2 to 3 mg/m^3 may produce irritation and discomfort. Above 3 mg/m^3 but below 25 mg/m^3, headache along with irritation is possible. Above 25 mg/m^3, additional neurotoxic effects may occur.[15] In all, studies by The National Institute for Occupational Safety and Health have shown that incidence of indoor air quality problems attributed to volatile chemicals is 4 times higher than problems attributed to micro-organisms.[16] Most VOCs originate from building materials such as carpet, insulation, adhesives, and sealants where methanol, HCHO, and a variety of organic solvents compose the off-gassing load. Likewise, the engine bleed from commercial aircraft that is used for cabin air makeup has been shown to contain VOC loading in the range of concentrations that contribute to irritation and discomfort.[17] While it is clear that the commercial and residential building industry can benefit from the lessons learned by NASA for minimizing chemical contaminant loading in buildings, the problem cannot be fully eliminated.[18] Similarly, commercial airliner engine bleed gases can only be so clean. Therefore, compact technologies that can help to control the remaining load will be instrumental in attacking this important environmental issue.

5. EXPERIMENTAL APPARATUS AND SUPPORT EQUIPMENT

Descriptions of the equipment used for conducting the experimental work are provided in sections 5.1 through 5.3. Primary equipment is based upon cabin air quality control systems used in NASA's crewed spacecraft to ensure that the USCM catalytic reactor evaluation results accurately reflect the actual performance in niche applications. Where necessary, equipment function and geometry are similar to equipment used on board the *ISS*.

5.1 Regenerative Life Support Equipment Test Stand

The regenerative life support equipment (RLSE) test stand (fig. 7) provided the working infrastructure for testing the USCM catalytic reactor. It contains an activated charcoal bed containing approximately 18.1 kg (40 lb) of Barnebey-Sutcliffe type 3032 activated charcoal, an axial blower, a centrifugal blower, a regenerable activated charcoal bed, an LiOH presorbent bed, a high-temperature catalytic oxidation (HTCO) assembly, a postsorbent bed containing approximately 1.4 kg (3 lb) of Cyprus Foote Mineral Co. LiOH, and associated instrumentation. Further details about the RLSE test stand are found in reference 19.

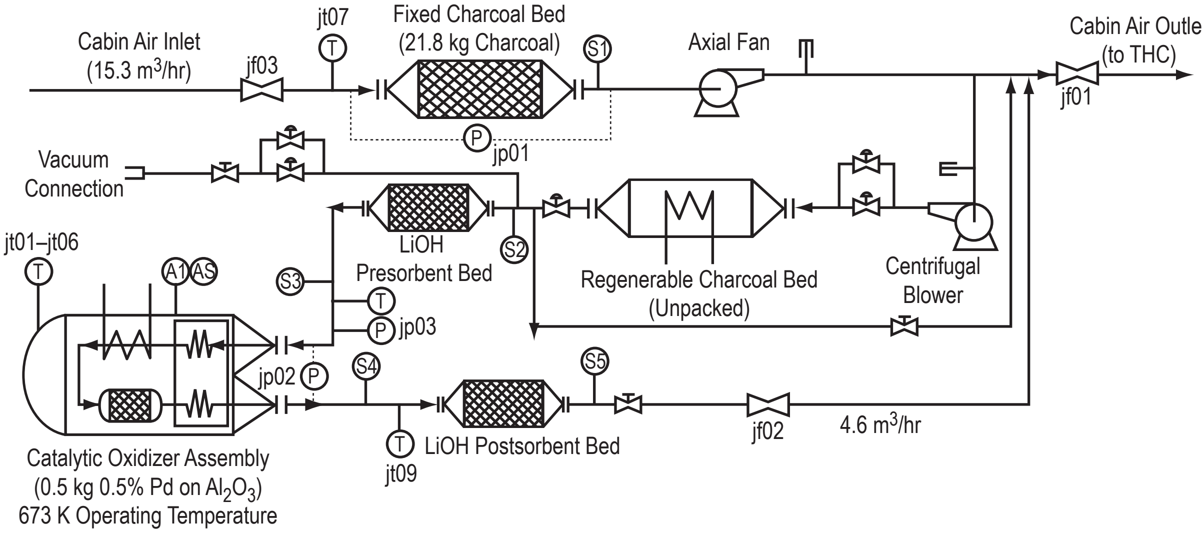

Figure 7. RLSE test stand process and instrumentation diagram.

For the purposes of the USCM catalytic reactor test project, the regenerable activated charcoal bed remained empty. The LiOH presorbent bed remained packed to serve as a static mixer for injected test gases. The TCO assembly was modified to accommodate the USCM catalytic reactor test article.

Process air enters the RLSE test stand directly from the facility high bay atmosphere. The test stand exhaust is vented from the high bay. Process gas flow through the test stand is regulated via hand valves. Fluid interfaces and process conditions are summarized in table 2.

Table 2. RLSE test stand fluid interfaces.

Fluid	Temperature (°C)	Pressure (kPa)	Flow Rate (m^3/hr)
Inlet air	18–27	100–102.7	15.3
TCO air	18–27	100	4.6
Exhaust air	49 maximum	100	15.3

5.2 Ultra-Short Channel Length, Monolithic Catalytic Converter Test Article

The USCM catalytic reactor test article shown in figure 1 was integrated into the existing RLSE test stand TCO assembly. Figure 8 shows the TCO assembly after its modification. Modification involved removing the existing catalyst bed and heater assembly. The USCM catalytic reactor assembly was inserted inside the large opening and then bolted into place.

Figure 8. RLSE test stand TCO with catalyst bed removed.

The USCM catalytic reactor test article is comprised of a catalyst/heater element assembly, a support structure, an interface adapter, and an end plate adapter containing instrumentation feedthroughs. Electrical wiring and instrumentation wiring are also a part of the assembly. Instrumentation is, at a minimum, in the form of thermocouples mounted at the inlet and outlet of the catalyst/heater element subassembly. Details on instrumentation locations are provided in appendix A. The USCM catalytic reactor operates on 120 V dc. Average power draw is 111.6 W. Maximum power is 166.7 W hot and 176.5 W cold. Electrical resistance ranges between 81 Ω cold and 84 Ω hot. On/off control of a variable voltage dc power supply was used to maintain the proper USCM catalytic reactor operating conditions.[20]

5.3 Support Equipment

The test facility provided a minimum complement of support capabilities. The capabilities contained in section 5.3 do not include any that were derived to meet other project requirements.

5.3.1 Contaminant Injection System

The capability was provided to inject selected chemicals into the RLSE test stand process air stream upstream of the LiOH presorbent bed as needed. This system was capable of injecting both liquid and gaseous chemicals to achieve a minimum 100 ±10 $\mathrm{ppm_v}$ concentration at the TCO assembly inlet. Contaminants injected are listed in table 3.

Table 3. USCM catalytic reactor contaminant challenge.

Compound	Molecular Weight (g/mole)	Inlet Concentration (mg/m^3)	Injection Rate* (mg/hr)
Isopropanol	60.09	246	1,451
Butanol	74.12	303	1,788
Acetone	58.08	238	1,404
Toluene	92.15	377	2,224
Methane	16.04	66	389
2-ethoxyethanol	90.12	369	2,177
Octafluoropropane	188.02	769	4,537
Sulfur hexafluoride	146.05	597	3,522

* At maximum USCM reactor flow condition of 5.9 m^3/hr.

Liquid contaminant injection was accomplished through the use of a syringe pump, and an additional low-flow air pump to provide flow into the oxidation loop of the test assembly. Gaseous contaminant injection was controlled by a programmable peristaltic pump. The gaseous contaminants were injected into the flow stream just upstream of the LiOH presorbent bed. The presorbent bed served as a static mixer in this application. Due to the higher injection rates allowed with pure gaseous contaminants—versus pure liquid, no additional air pump was required for gaseous contaminant injection.

5.3.2 Process Gas Sample Collection and Analysis Equipment

Equipment was provided to collect and analyze process gas samples using in-line techniques. CO_2 in both the TCO assembly inlet and outlet was analyzed with a Horiba model VIA–510 CO_2 gas analyzer unit. The CO_2 analyzer was connected to a Horiba general purpose sample unit model ES–C510E used to condition the sample before analysis. Oxidation efficiencies were calculated based on differential CO_2 concentration and material balance calculations.

5.3.3 Uninterruptable Power Supply

An uninterruptable power supply (UPS) was provided to the RLSE test stand to allow for a graceful shutdown in the event of a facility power failure.

5.3.4 Instrumentation

The instrumentation listed in table 4 was provided to achieve the project objectives. Existing instrumentation used during previous Environmental Control and Life Support System (ECLSS) testing was used. Details on the instrumentation contained within the USCM catalytic reactor assembly are provided in appendix A.

Table 4. Experimental apparatus instrumentation.

Parameter	Units	Range
High bay CO_2 partial pressure	%/mm Hg	0–1 / 0–5
Catalytic oxidizer delta pressure	inches H_2O	0–10
USCM reactor voltage	V	0–120
USCM reactor current	A	0–20
Catalytic oxidizer inlet temperature	°F	50–120
Pre-USCM reactor temperature*	°F	50–800
Post-USCM reactor temperature*	°F	50–900
Post-USCM reactor air gap temperature*	°F	50–900
Hot side heat exchanger inlet temperature*	°F	50–900
TCCS HTCO feedthrough temperature	°F	50–200
Catalytic oxidizer exhaust temperature	°F	50–200
Test stand inlet air temperature	°F	50–90
Test stand inlet airflow rate	scfm	0–20
Catalytic oxidizer assembly airflow rate	scfm	0–5
Contaminant injection rate	scim	0–30

* See appendix A for thermocouple locations.

5.3.5 Control and Data Acquisition

LabView® data acquisition software was used for test apparatus command and control for this test. Data archiving was provided by the Marshall Payloads and Real-time Automated Test System (PACRATS) data archiving system. PACRATS provided the ability to recall all data and make plots of specific instrument readings.

5.3.6 Documentation

A logbook was kept during the metal monolith performance demonstration project. Details on the metal monolith catalytic converter integration and test events such as startup, shutdown, mode changes, anomalies, and all other relevant activities were recorded for purposes of correlating with test data. Logbook entries included the date, time, and initials of the person making the entry in addition to a detailed description of the event.

In the event of a system or subsystem test anomaly, a complete description of the problem was recorded in the logbook. The description defined the anomaly, date and time, the procedures used to correct the anomaly, and the outcome.

6. TEST ARTICLE INTEGRATION AND EXPERIMENTAL APPROACH

The USCM catalytic reactor performance evaluation was conducted in two phases. The first phase addressed the physical integration of the USCM test article with the RLSE test stand TCO assembly recuperative heat exchanger as well as the mechanical, electrical, and instrumentation checkout of the fully integrated unit. The second phase addressed the performance and energy requirements of the test article.

6.1 Test Article Integration and Checkout

Before testing began, the USCM catalytic reactor assembly was installed into the existing RLSE TCO assembly. The physical installation was verified by inspection. All mechanical, fluid, electrical, data acquisition, and control interfaces were verified by inspection and demonstration.

6.1.1 Ultra-Short Channel Length, Monolithic Catalytic Reactor Assembly Integration

The USCM catalytic reactor assembly was inserted into the opening in the TCO assembly that previously held the catalyst bed and heater assemblies shown in figure 8. Before integration occurred, the RLSE test stand TCO was disconnected from all electrical power and instrumentation. The integration of the USCM catalytic reactor with the TCO recuperative heat exchanger assembly was conducted in a shop area located in building 4755 at NASA Marshall Space Flight Center.

Care was taken to maintain in place all insulating materials directly surrounding the heat exchanger and reactor assembly. This insulation is Johns Manville Q-Fiber® felt. The TCO assembly's external insulation, however, was asbestos based and was replaced with new asbestos-free Wrap-It 372 moldable ceramic mat insulation manufactured by Cotronics Corporation, Brooklyn, NY. The Wrap-It 372 insulation is a similar material with better insulating properties than Manville's Q-Fiber felt. Properties of both the Manville and Cotronics insulation products are provided in table 5. A layer of aluminum foil was also added as a radiant barrier beneath the moldable insulation and on the outside of the entire TCO assembly.

The USCM catalytic reactor assembly shown in figure 1 was inspected and photographed before integration with the recuperative heat exchanger assembly. All seals used with the original configuration were cleaned before reuse. The small diameter, stainless steel seal was installed over the corresponding diameter knife-edge channel on the forward wall of the catalyst basket retainer shown in figure 8. The K-ring seal was placed on the end flange. The USCM catalytic reactor assembly, including end plate, was then inserted into the catalyst bed retainer. Its forward adapter is in contact with the forward stainless steel seal. Light pressure was applied to the end plate to check proper clearances. Appropriate adjustments were made to ensure a tight seal was provided by the K-ring and to prevent damage to the catalytic reactor assembly. Once a proper fit was obtained, the end plate was bolted to the TCO assembly flange. The assembly was then installed in the RLSE test stand and prepared for checkout. This successful integration fully demonstrated the feasibility for retrofitting the TCO assembly in the *ISS* TCCS with

Table 5. TCO assembly insulation properties.

Property	Value
Manville Q-Fiber Felt	
Nominal thickness	0.5 in
Nominal density	6 lb/ft^3
Nominal weight	0.25 lb/ft^2 ± 10%
Linear shrinkage	$\leq$0.7% at 1,000 °F
Thermal conductivity at 300 °F	0.3 Btu-in/ft^2·hr·°F
Thermal conductivity at 700 °F	0.5 Btu-in/ft^2·hr·°F
Thermal conductivity at 1,000 °F	0.68 Btu-in/ft^2·hr·°F
Cotronics Wrap-It 372	
Nominal thickness	0.5 in
Nominal density	18 lb/ft^3
Linear shrinkage	2% at 2,200 °F
Thermal conductivity at 1,000 °F	0.7 Btu-in/ft^2·hr·°F

a USCM reactor assembly. A photographic record of the installation process (fig. 9) was obtained of the integration operation. Note the yellow fiberglass insulation depicted in the photos was found to be inadequate and was replaced with Cotronics Wrap-It 372 moldable ceramic mat insulation described above.

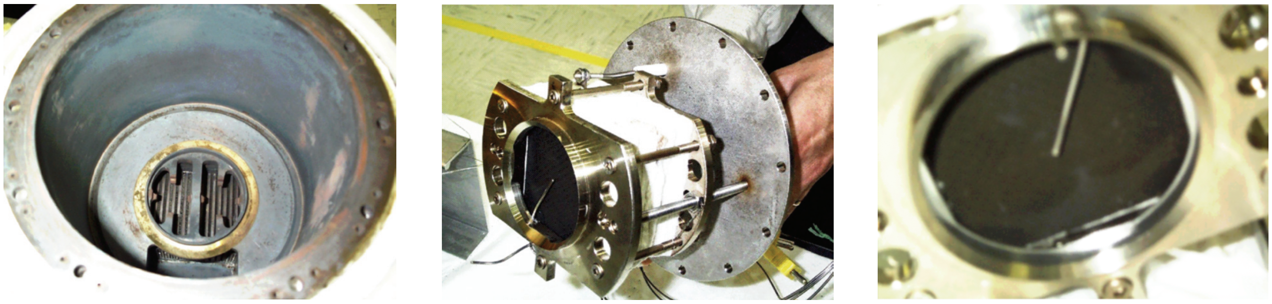

Recuperative Heat Exchanger Assembly
(a)

USCM Reactor Assembly
(b)

Knife-Edge Detail
(c)

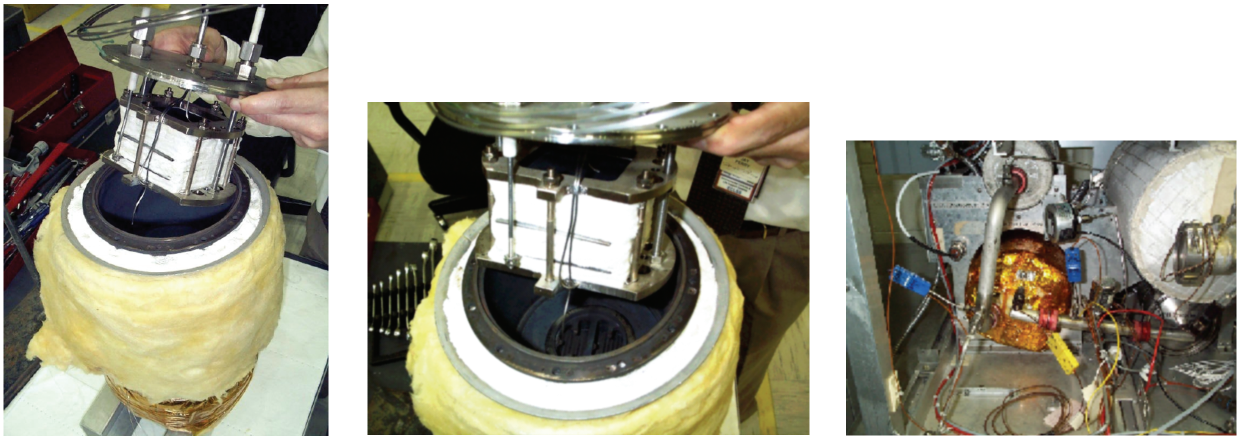

Orienting the USCM
(d)

Inserting the USCM
(e)

Overall Test Bed
(f)

Figure 9. USCM reactor assembly installation shown in (a)–(f).

6.1.2 Mechanical, Electrical, and Instrumentation Checkout

The mechanical installation and all electrical and instrumentation connections and function was verified by visual inspection and demonstrated before performance testing. The mechanical installation was verified by conducting a leakage check at the rear flange of the catalytic oxidizer assembly as 4.6 m^3 process air/hour (2.7 cfm) flowed through it. Power was applied to the USCM catalytic reactor during checkout to determine if any leakage occurs due to thermal effects. No leaks were observed.

The electrical and instrumentation connections were verified by visual inspection and by demonstrating control connectivity. The USCM reactor cold resistance was measured before and after installation in the TCO assembly. Proper function was demonstrated by commanding the TCO assembly through a normal startup and shutdown sequence with 1 hr of normal operations between the startup and shutdown commands. Normal operating conditions for the purposes of the checkout are 4.6 m^3 process air/hour and 400 ± 5.6 °C (750 ± 10 °F).

6.2 Ultra-Short Channel Length, Monolithic Catalytic Reactor Performance Evaluation Approach

Testing the prototype USCM catalytic reactor was accomplished according to the following plan.

6.2.1 Process Characterization

The USCM reactor process was characterized under varying process airflow and electrical power input conditions. The maximum electrical power applied to the USCM catalytic reactor was 120 V dc. The voltage was regulated to achieve varying power input to the USCM reactor.

Table 6, a $4^1 \times 5^1$ orthogonal array, summarizes the test runs performed. Once oxidation was shown not to occur at a particular airflow or power rating, the tests to be performed at higher airflow settings or lower power settings were deleted from the matrix. Test runs at 1.7-m^3 process air/hour flow conditions contained in the original test plan were deleted from the procedure after it was found that contaminant injection was difficult to control, making useful data acquisition all but impossible.

Process parameters consisting of the peak power, average power, maximum process temperature, and TCO assembly pressure drop at the maximum process temperature were recorded for each run. The initial test plan called for all runs to start from ambient temperature conditions. It was later decided to modify settings for contaminant oxidation runs without going through a cooldown period. Temperature ramp tests were conducted as a separate phase of the overall test plan.

For the temperature ramp runs, electrical power was applied to the USCM catalytic converter to raise its temperature from ambient to the maximum temperature noted for each run. The rate of temperature rise of the USCM reactor assembly was monitored. The elapsed time to reach a steady temperature condition for the metal monolith catalytic reactor and the heat exchanger assembly was recorded. Once the average change in the USCM reactor assembly outlet temperature measurement was less than 0.3 °C/hr (0.5 °F/hr), the power was shut off. Both RLSE test stand fans remained on for at least 2 hr during the cooldown period or until the USCM reactor outlet air temperature reading fell below 149 °C (300 °F).

Table 6. Process characterization test runs.

Run	Process Flow (m^3/hr)	Power Input (% of Maximum)
1*	1.7	100
2*	1.7	75
3*	1.7	50
4*	1.7	25
5	3.4	100
6	3.4	75
7	3.4	50
8	3.4	25
9	4.6	100
10	4.6	75
11	4.6	50
12	4.6	25
13	5.1	100
14	5.1	75
15	5.1	50
16	5.1	25
17	5.9	100
18	5.9	75
19	5.9	50
20	5.9	25

* Run not conducted due to contaminant injection control limitations.

6.2.2 Contaminant Oxidation Performance

The test conditions from table 5 were repeated using each of the contaminant challenges listed in table 3. Before applying power to the USCM reactor, the baseline CO_2 concentration at the TCO assembly inlet and outlet was measured. After applying power to the TCO assembly, the contaminant injection began once the USCM reactor assembly reached maximum temperature. This is defined as a USCM reactor assembly outlet temperature rate of change less than 0.3 °C/hr (0.5 °F/hr). CO_2 was monitored in the TCO exhaust air for several minutes so that a reasonable data set could be obtained. Due to time constraints, one test run for each contaminant was completed.

For the cases involving octafluoropropane (C_3F_8) and sulfur hexafluoride (SF_6), CH_4 oxidation performance was measured immediately after stopping the contaminant injection. This was done to determine whether any catalyst poisons were generated during the run.

6.2.3 Durability Characterization

A final extended-duration performance test was conducted at the optimum process conditions indicated by the performance characterization testing. CH_4 was injected periodically during the test at a rate sufficient to provide 65 ± 7 mg/m^3 (100 ± 10 ppm_v) at the TCO assembly inlet. CO_2 concentration at the TCO assembly exhaust was monitored to determine CH_4 oxidation performance. The durability characterization run will continue for a minimum of 8 wk and a maximum of 104 wk. The objective of this run is to understand the long-term operational characteristics of the USCM reactor assembly.

7. EXPERIMENTAL PROCEDURES

Special experimental procedures were limited to gaseous and liquid contaminant injection and CO_2 monitoring.

7.1 Gas Injection

In order to inject the contaminant gas just upstream of the LiOH bed, a programmable peristaltic pump was used. Once the temperature was reached and stable for the given power and flow setting, the injection line was connected to the gasbag and then purged. After setting the required injection rate, samples were pulled after 10 min and then again at 30 min. Samples were taken by a Horiba infrared CO_2 analyzer, which monitors CO_2 in parts per million. By changing the sample port from inlet to outlet, a comparison of CO_2 concentration was used to determine if the metal monolith was oxidizing the contaminant.

7.2 Liquid Injection

Liquids were injected by means of a syringe pump, which allowed for a very low injection rate. In order to have the contaminant in gas form, a heater was connected to allow the liquid to vaporize at the injection point. Once the injection rate began, samples were pulled with a Horiba infrared CO_2 analyzer, as with the contaminant gases. However, before samples were taken, the liquid was allowed to run through the system ≈1 hr to allow the oxidation to stabilize.

7.3 Modified Injection Assembly

The contaminant gas injection ran according to procedure. There were no problems detecting the oxidation if it occurred.

The liquid contaminants were more difficult to inject for maximum oxidation efficiency measurements at the low process airflow conditions. The injection setup was supposed to cause the liquid to flash boil at the point of injection. At lower airflow conditions, the liquid formed a droplet that did not fully evaporate and eventually swept from the injector as a large pulse. This caused large fluctuations in the outlet CO_2 concentration measurements. In order to alleviate this problem, a heater was added to the point of injection and the injection rate was decreased on 10-percent intervals until the injection became more uniform.

Initially, there were problems detecting oxidation for some of the liquids expected to oxidize fairly easily. A hypothesis for this difficulty was injection leakage; investigation confirmed the hypothesis. The rubber tubing connecting the syringe to the injection piping was found to react with the liquid solvent contaminants, become gummy, and eventually break. Various pieces were used to attach the syringe to the piping, but they leaked or broke on more than one occasion, leading to poor liquid contaminant injection control. Finally, a polypropylene luer to 1/8-in compression fitting was used with the luer end connecting to the syringe and the compression side connected directly to the 1/8-in stainless steel piping, which proved to work well with no leakage.

8. RESULTS AND DISCUSSION

Experimental data were acquired on CH_4, C_3F_8, SF_6, and non-CH_4 VOC oxidation; reactor thermal response; pressure drop; and electrical power duty. Data were reduced to investigate performance trends under the experimental conditions. These trends are presented in the following discussion. Tabular-reduced data are provided in appendix B.

8.1 Gaseous Contaminant Oxidation

Representative chemical contaminants were injected into the process air stream entering the USCM catalytic reactor. These contaminants included CH_4, acetone, n-butanol, ethoxyethanol, isopropanol, toluene, C_3F_8, and SF_6. Of these, SF_6 was the only chemical challenge that showed no direct indication of oxidation. CH_4, C_3F_8, and SF_6 are presented individually while the remaining compounds are grouped as non-CH_4 VOCs.

8.1.1 Methane Oxidation

CH_4 is a key design-driving challenge for spacecraft thermal catalytic oxidation processes. For applications that require high single-pass efficiency, a catalytic reactor's performance for CH_4 oxidation is central to specifying the temperature conditions. CH_4 oxidation performance for the range of process flow conditions investigated is presented in figure 10. Oxidation efficiency tends to be insensitive to flow rate with the reaction lighting off at 240 ºC. This is comparable to, but less active than, indirectly heated, pellet-supported platinum group metal catalysts in use on board the *ISS*.[21,22]

Experimental runs using different combinations of power applied to the reactor and process flow rate show that the best performance occurs when maximum temperature can be maintained in the reactor. This typically occurs at low process airflow rate and high-power application conditions, as shown in figure 11. The best overall performance is obtained when applying 160 W. CH_4 oxidation drops quickly for lower power settings as process airflow increases.

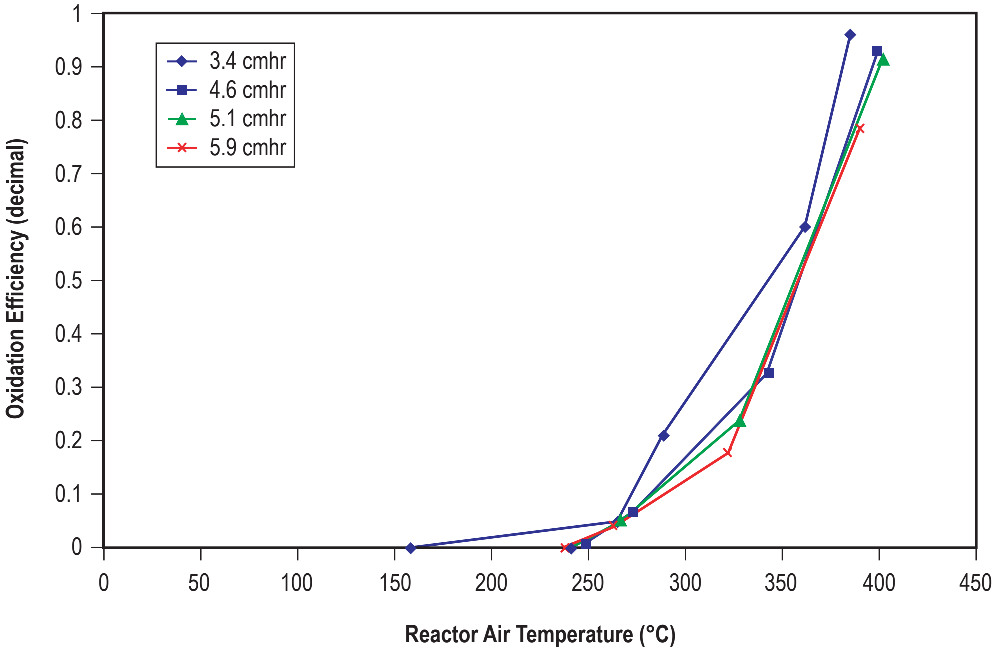

Figure 10. CH_4 oxidation efficiency.

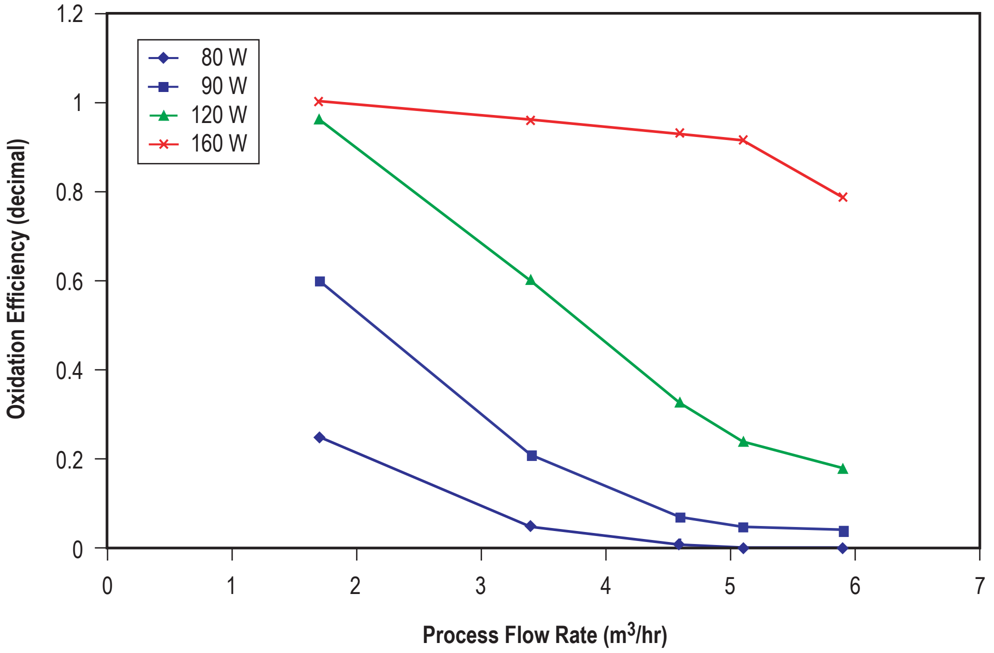

Figure 11. CH_4 oxidation efficiency at varying power and flow conditions.

Figure 12 compares the observed CH_4 oxidation efficiency for the USCM reactor to a subscale reactor containing 0.5 percent Pd on Al_2O_3 pellets. Palladium supported on Al_2O_3 has been the performance standard that NASA uses for evaluating emerging thermal oxidation technologies. As figure 12 shows, the Pd catalyst under flow conditions producing 8,000 hr^{-1} gas hourly space velocity (GHSV) possesses a lower light-off temperature than the USCM reactor operating at 9,141 hr^{-1} GHSV. These flow conditions are the closest available for comparative purposes. The USCM reactor's light-off temperature under these conditions is 20 percent greater than the Pd on Al_2O_3 pellets. However, the USCM reactor's residence time is 14 percent lower. Given the USCM reactor's light-off temperature consistency between 240 and 250 ºC shown in figure 10, it is concluded that the catalyst supported on the USCM substrate is less active than Pd supported on Al_2O_3 pellets. Since one expects space velocity and reaction rate to be inversely proportional for the elementary first-order CH_4 oxidation reaction, this can, in theory, be compensated for by operating at lower flow conditions or increasing the reactor volume. Figure 12 shows the performance difference becomes less at full-up operating conditions, making the time to reach that condition more important, thus making the thermal response of the two reactors an important distinguishing characteristic.

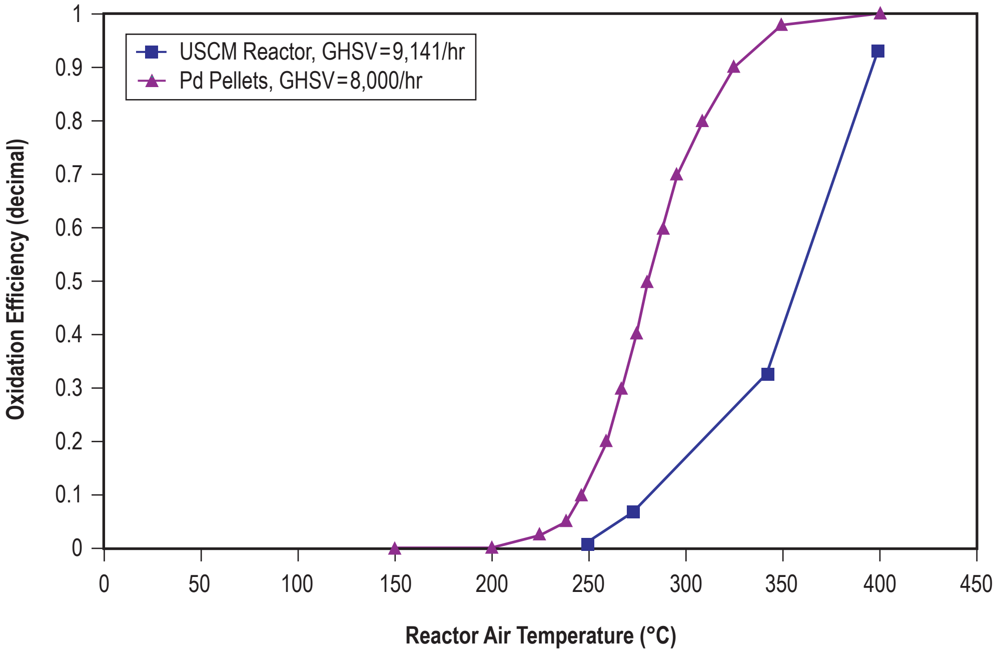

Figure 12. CH_4 oxidation over USCM- and pellet-supported catalysts.

8.1.2 Octafluoropropane Oxidation

Halocarbon oxidation is a challenge for thermal catalytic oxidation processes. First, halogen atoms are strongly bound to the molecule's carbon atoms and require a large amount of energy to break the bonds. Therefore, oxidation efficiency is typically much lower than for CH_4 in the range of process temperatures. Second, halogens can poison a catalyst. Previous work has shown CH_4 oxidation efficiency losses of 90 percent, depending on the halocarbon compound and its concentration in the process air entering the reactor.[23] CH_4 oxidation light-off temperature for a poisoned catalyst can increase by 100 ºC or more. For this reason, most process gas decontamination systems that employ thermal catalytic oxidation have some pretreatment stage to remove catalyst poisons or the reactor is overdesigned to accommodate the poisoning effect. The poisoning effects, however, can be almost completely reversed by purging the reactor with clean gas.[24,25]

Fortunately, halocarbon use in manufacturing has become less common as environmental friendly chemicals replace halocarbons. However, some fully fluorinated hydrocarbons—perfluorocarbons and perfluoroalkylethers—are either used as thermal control system working fluids or are under consideration. C_3F_8 is a perfluorcarbon used on board the *ISS* as a thermal working fluid. Previous testing shows C_3F_8 is not oxidized to a measurable extent over platinum group metal catalyst on Al_2O_3 pellets.[26] Comparatively, the USCM catalytic reactor exhibited greater activity than platinum group metal catalyst on Al_2O_3. Figure 13 shows reaction light-off above 275 ºC.

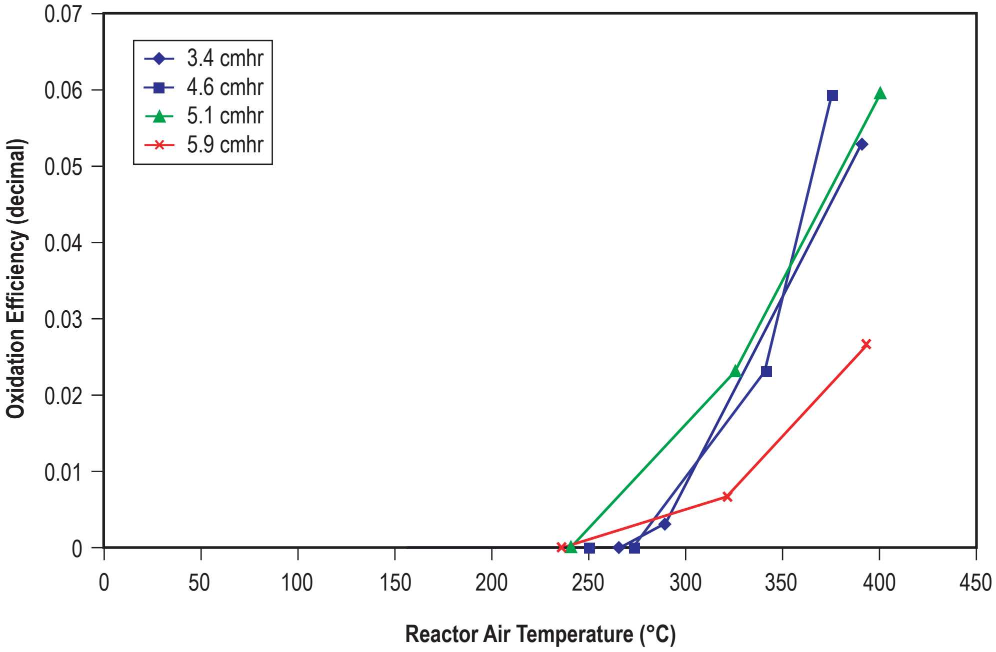

Figure 13. C_3F_8 oxidation efficiency.

CH_4 oxidation performance was checked before and after the C_3F_8 challenge runs. No indication of catalyst poisoning was noted. Poisoning resistance is an important distinguishing feature because the pellet-supported Pd catalyst used on board the *ISS* is susceptible to poisoning by halocarbons. While typical concentrations in most indoor air quality applications are barely detectable, more detailed testing will be required for niche applications that may experience high halocarbon concentration.

8.1.3 Sulfur Hexafluoride Oxidation

SF_6 is commonly used in combustion-related payloads as an inert blanketing gas. When such payloads have been on board the Shuttle or Spacelab, measurable quantities have been found in the cabin atmosphere. Because sulfur-containing compounds are known to be strong, irreversible catalyst poisons, the effects SF_6's presence may have on CH_4 oxidation efficiency were investigated. Experimental runs using only CH_4 as the reactor challenge were conducted before and after injecting SF_6. The experimental runs to investigate SF_6 oxidation revealed no directly measurable evidence to indicate it was destroyed in the reactor. This conclusion is supported by the observation that CH_4 oxidation performance before and after injecting SF_6 into the reactor was unchanged.

Extending this part of the investigation, SF_6 and CH_4 were injected simultaneously to determine whether SF_6's mere presence can alter the reactor's CH_4 oxidation performance. This experimental run noted a 26-percent reduction in CH_4 oxidation efficiency when SF_6 was present. CH_4 oxidation efficiency recovered once the SF_6 cleared from the reactor. This reversible effect further indicates SF_6 is not oxidized. However, there is interaction with the catalyst surface, inhibiting CH_4 oxidation—most likely physical adsorption.

8.1.4 Nonmethane Volatile Organic Compound Oxidation

Oxidation reaction light-off for non-CH_4 VOCs was found to occur near 150 ºC. Figure 14 shows the composite non-CH_4 VOC oxidation results. Data clusters fairly well for the higher flow rate conditions while lower flow rate conditions indicate more scatter. The scatter for the 3.4-m^3/hr and 4.6-m^3/hr flow conditions is particularly evident in the lower right quadrant of figure 14. As related earlier, achieving uniform liquid contaminant injection under low flow conditions was a challenge. The scatter in oxidation performance under the lower flow conditions is attributed to the contaminant injection difficulties.

Taking the injection difficulties into account, the data clusters appear to fall along an S-shaped curve. Such a response is typical for thermal catalytic oxidation reactors in use on board the *ISS*. By averaging the oxidation efficiency versus temperature data and dropping the outlying data, the fit to an S-shaped curve is more evident, as figure 15 shows. The S-shaped curves displayed in figures 14 and 15 are not regression curves and are for reference only. The averaged data can be fit to a third-order polynomial with a high degree of correlation, giving further evidence for an S-shaped oxidation response curve.

Both figures 14 and 15 show a data gap between 200 and 275 ºC. Interpolation indicates expected efficiency in this range is 30 to 70 percent. While more experimental runs with improved injection control are required to fill the gap, testing conducted by NASA Glenn Research Center (GRC) using a similar USCM reactor with no recuperative heat exchanger reported oxidation efficiencies between 35 and 65 percent.[27] Early developmental work by PCI indicates that the reactor outlet temperature can be increased by $\approx$0.4 ºC for each degree that the inlet gas stream is elevated above ambient temperature (20 ºC basis).[28] Therefore, the expected air temperature exiting the reactor under the conditions evaluated by GRC is expected to be 100 to 200 ºC lower than what can be achieved with a recuperative heat exchanger. Under such conditions, the reactor temperature is expected to range between 200 and 300 ºC. Non-CH_4 VOC oxidation performance observed during the GRC evaluation is consistent with the oxidation efficiency expected from interpolation of results documented by figures 14 and 15.

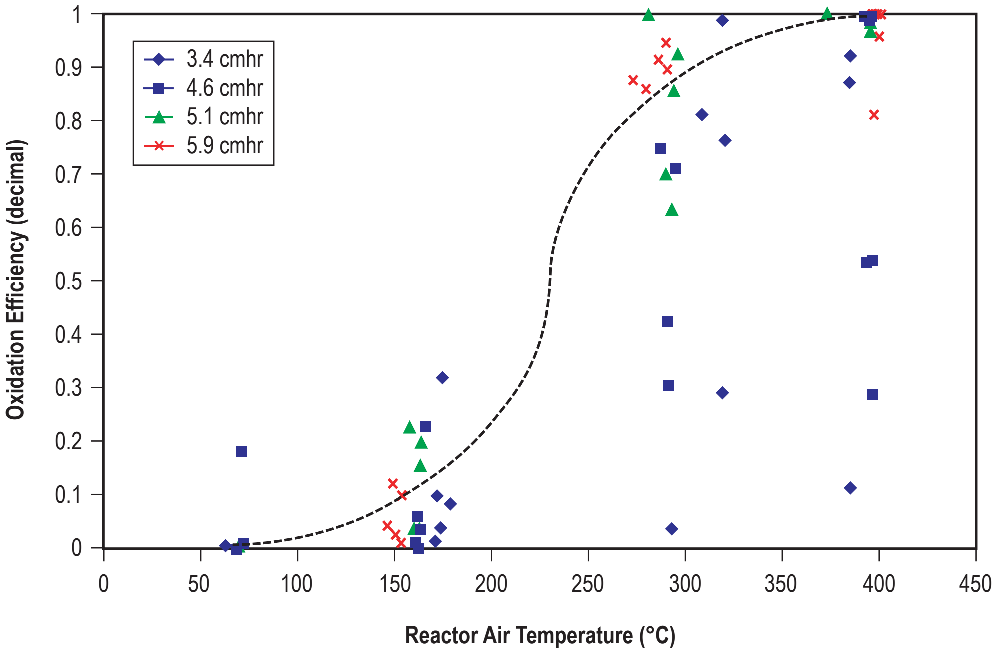

Figure 14. Composite non-CH_4 VOC oxidation performance.

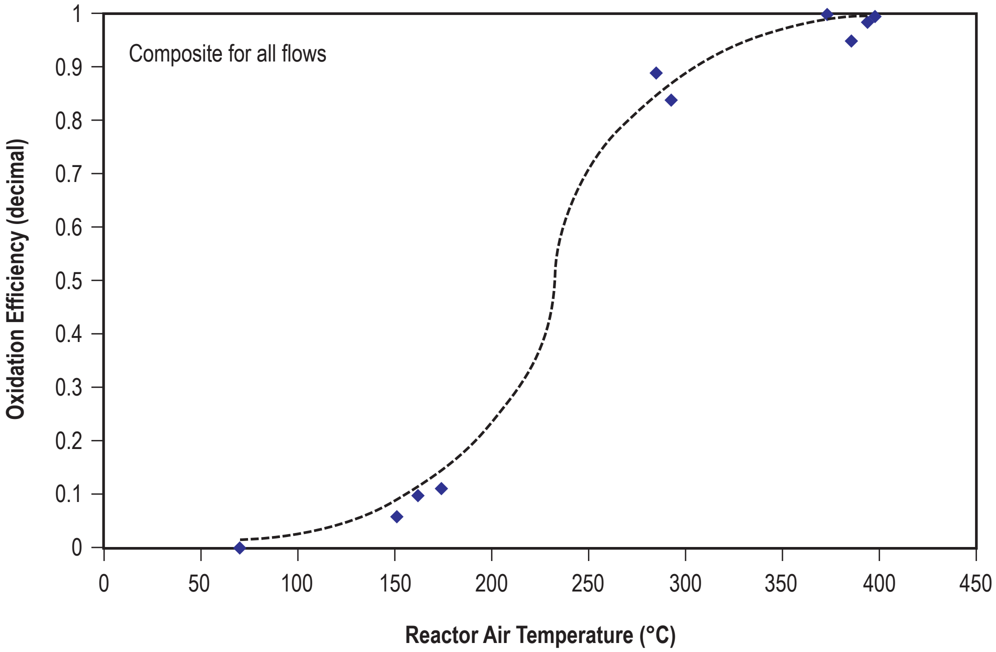

Figure 15. Averaged non-CH_4 VOC oxidation performance.

Figure 16 shows a very interesting relationship between non-CH_4 VOC oxidation efficiency and process flow conditions. As the process airflow approaches 3 m^3/hr, oxidation efficiency increases. At flow conditions >3 m^3/hr, the oxidation efficiency tends to decrease. This phenomenon is thought to result from the enhancement of the mass transfer coefficient provided by the USCM substrate. Because the oxidation reaction is diffusion limited, enhancing the mass transfer coefficient can improve performance. Increasing the process airflow rate achieves this result. However, a flow condition is ultimately reached where shorter residence time negates the mass transfer enhancement. At that point, reaction kinetics becomes dominant and oxidation efficiency decreases as the residence time decreases. This appears to occur for the USCM reactor tested at process airflow conditions >3 m^3/hr.

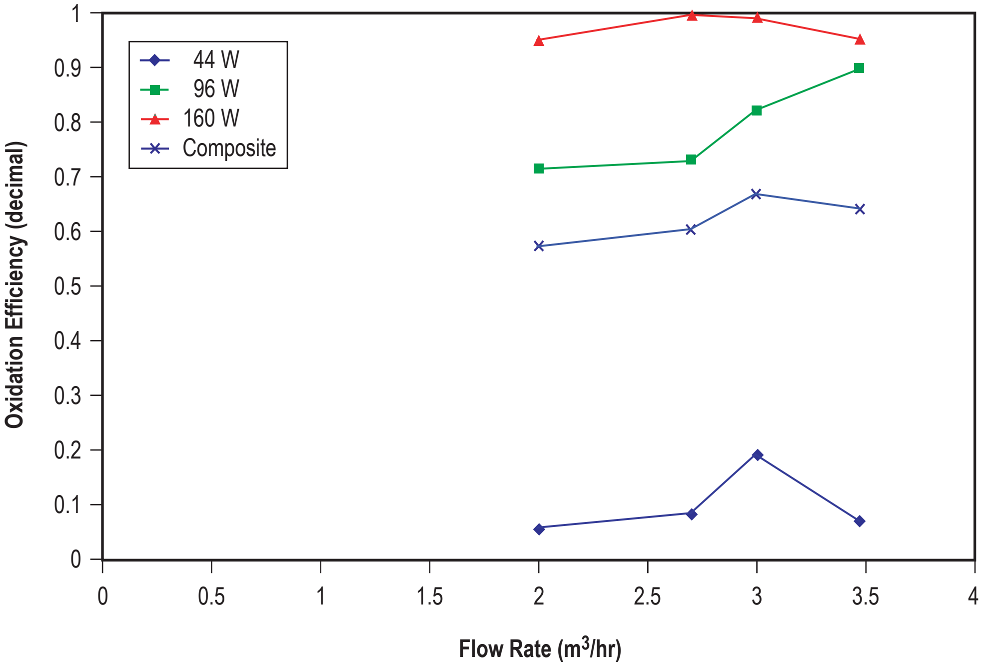

Figure 16. VOC oxidation efficiency at varying power and flow conditions.

8.2 Reactor Thermal Response

The USCM-based reactor's thermal response, when combined with oxidation performance, provides the necessary data for establishing operating conditions for niche applications. Steady state and transient conditions were addressed by the experimental runs.

8.2.1 Maximum Process Air Temperature

Maximum process air temperature was found to be influenced by both process airflow rate and power input. As figure 17 shows, the highest steady state process temperature is achieved for the combination of low flow rate and high power input. All flow conditions converge on 400 ºC as the maximum steady state temperature condition because heater control cycled off after reaching 404 ºC and on after reaching 393 ºC. The deadband power control causes the steady state temperature curve for the 1.7-m^3/hr

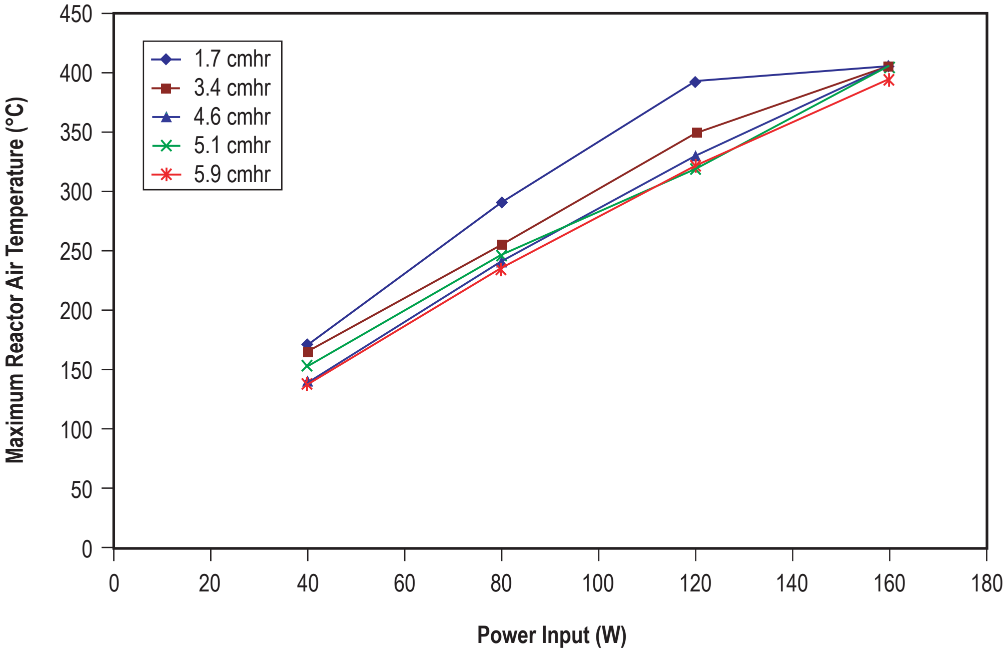

Figure 17. Maximum achievable reactor temperature.

flow case to lie over. The deadband control effect becomes less pronounced as process airflow increases and the applied power becomes less able to overcome convective energy losses. Discounting the deadband control effect and extrapolating the 1.7-m^3/hr case indicates a maximum steady state temperature just over 500 ºC when applying 160 W. Similar extrapolation can be made for the other low flow rate conditions to account for the control deadband. It should be noted that the control deadband was selected not only to provide a comparison with existing thermal catalytic reactors used on board the *ISS* but also to avoid damaging the USCM substrate and catalytic coating. Destructive testing to understand the absolute temperature limit for the USCM substrate and catalytic coating was not attempted because only one reactor was available for experimentation.

8.2.2 Elapsed Time to Methane and Volatile Organic Compound Oxidation Light-Off

Another measure of the USCM catalytic reactor's performance is how much time elapses from cold startup to when it begins to actually function; i.e., how long does it take before the oxidation reaction initiates. Figures 18 and 19 illustrate the elapsed time to achieve CH_4 oxidation reaction and non-CH_4 VOC oxidation reaction light-off.

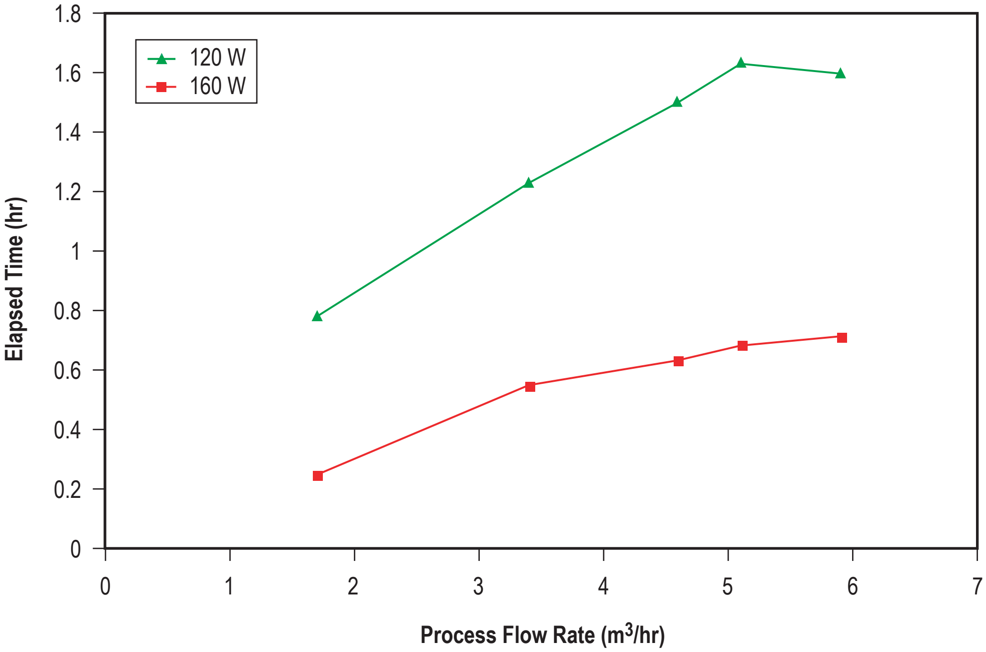

Figure 18. Elapsed time to CH_4 oxidation light-off.

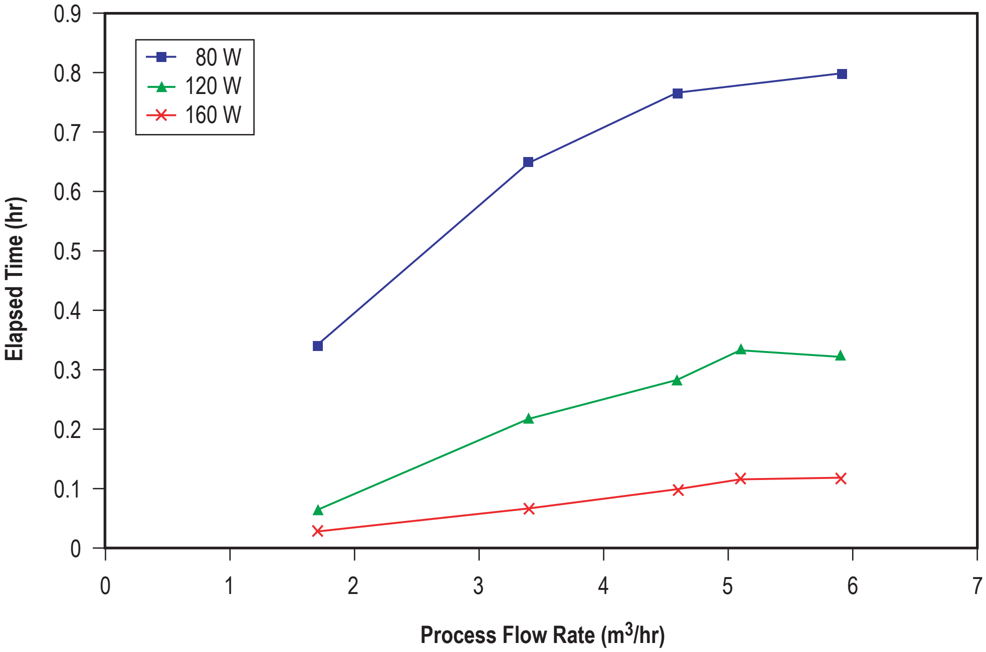

Figure 19. Elapsed time to non-CH_4 VOC oxidation light-off.

To oxidize CH_4, at least 120 W applied power is necessary for the elapsed time to be less than the >1.7 hr required for existing thermal catalytic reactors on board the *ISS* to become fully operational. Data indicate the USCM catalytic reactor can reduce the elapsed functional startup time by 12 percent while using 25 percent less power. Using the same power as equipment on board the *ISS*, elapsed functional startup time is reduced by nearly 63 percent.

If CH_4 oxidation is not required for a niche application, the time to functional startup, shown in figure 18, is more rapid. As expected, the greater the applied power, the shorter the elapsed functional startup time. For non-CH_4 VOCs, functional startup can be achieved in <1 hr for applied power as low as 80 W. Using 160 W, functional startup can be achieved in <7 min for all flow rate conditions investigated.

8.2.3 Elapsed Time to Complete Startup

Complete startup is achieved by reaching the peak control deadband temperature. The thermal catalytic reactor used on board the *ISS* requires 3 hr to reach 400 ºC using 160 W power input. The flow condition is 4.6 m^3/hr. By comparison, when outfitted with a bed of catalyst pellets and immersion heater assembly, the catalytic reactor used as the basis for the USCM reactor performance characterization requires >8 hr to achieve complete startup under comparable flow conditions using 140 W power input.[29] This demonstrates significant differences between the thermal mass and insulation of the catalytic reactor used for experimental testing and the flight version. These differences imply greater energy loss from the experimental reactor leading to greater power and longer elapsed time to achieve thermal steady state.

Replacing the bed of catalyst pellets and immersion heater assembly with the USCM catalytic reactor assembly, along with applying insulation to the TCO assembly's exterior, resulted in significantly reduced elapsed startup time. Figure 20 shows startup duration just over 3.5 hr for the 4.6-m^3/hr flow condition with 160 W power input. This represents a >56 percent improvement compared to the same TCO assembly outfitted with the bed of catalyst pellets and immersion heater assembly. The performance is comparable to the flight TCO assembly. Although direct comparison to the flight TCO assembly is difficult and the degree of improvement cannot be quantified without direct retrofit, it is reasonable to expect shorter elapsed time for complete startup based on the experimental results.

8.3 Pressure Drop

Both temperature and process airflow influence the overall TCO assembly pressure drop. Most flow conditions investigated maintained pressure drop <1 kPa for the entire range of process air temperature as shown in figure 21. Pressure drop exceeding 1 kPa was measured for the 5.1 m^3/hr flow condition when the process temperature exceeded 300 ºC. Likewise, 1 kPa pressure drop was exceeded above 200 ºC for the 5.9-m^3/hr flow condition.

Comparison of the USCM reactor assembly pressure drop to the original fixed pellet bed is accomplished by evaluating original design data for the TCO assembly. As originally designed, the total TCO assembly pressure drop was 2,320 Pa at 5.6 m^3/hr and 360 ºC. The catalyst bed design, containing 3.175-mm cylindrical pellets, contributed 523 Pa to the overall TCO assembly pressure drop at this flow condition.[30] From this, the heat exchanger subassembly and various duct losses can be estimated to contribute up to 1,790 Pa, or 77 percent of the total TCO assembly pressure drop.

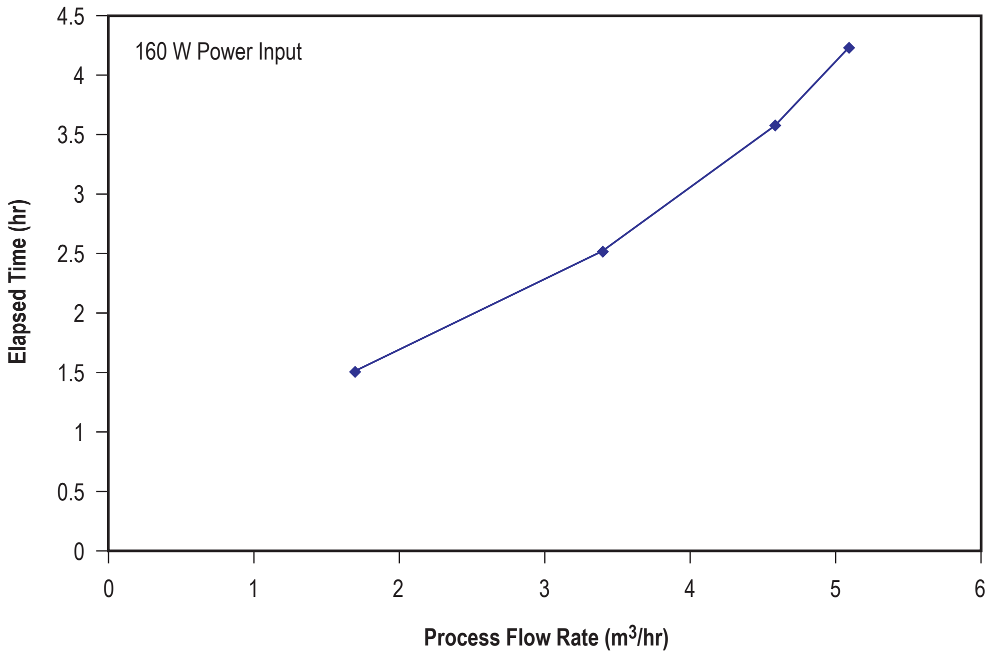

Figure 20. Elapsed time to complete startup.

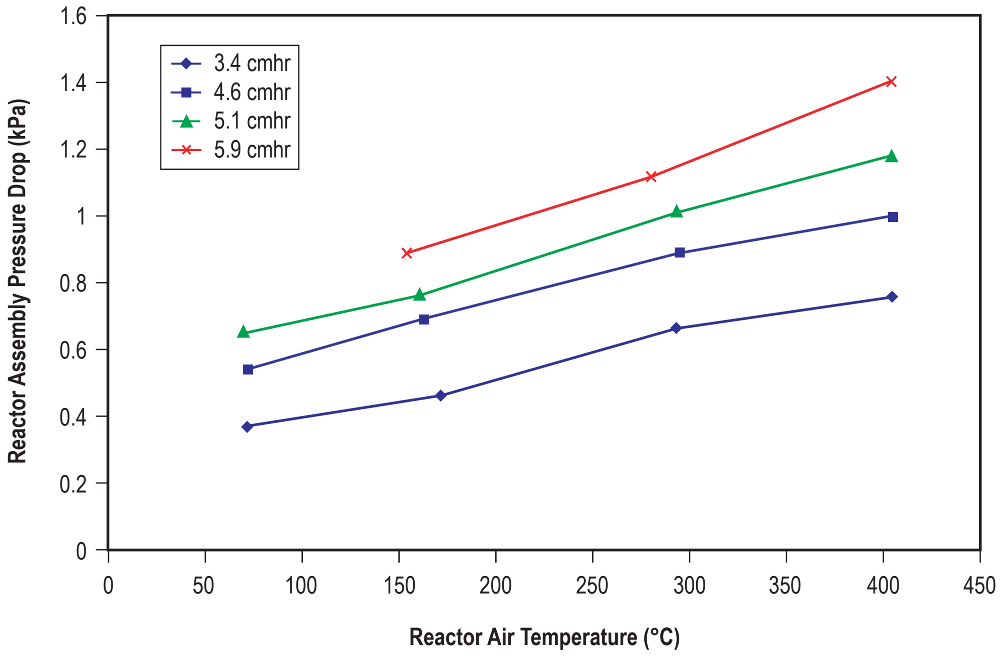

Figure 21. Effects of temperature on TCO assembly pressure drop.

For testing with the USCM reactor in place of the pellet bed, the highest flow rate used was 5.9 m^3/hr. This is very close to the original TCO assembly design condition. The pressure drop measured under this flow condition at 400 ºC was 1,407 Pa. Assuming the heat exchanger assembly's percentage contribution to overall pressure drop remains unchanged across the range of flow conditions for a single temperature, the data and regression equation of figure 22 can be used to estimate the USCM reactor assembly's pressure drop. By this technique, the heat exchanger subassembly and duct losses account for 77 percent of the total TCO assembly pressure drop. This places the USCM reactor assembly pressure drop in the range of 174 to 324 Pa for the process flow rates ranging between 3.4 and 5.9 m^3/hr. Compared to the original pellet bed design, the USCM reactor can be expected to provide up to 38 percent lower pressure drop.

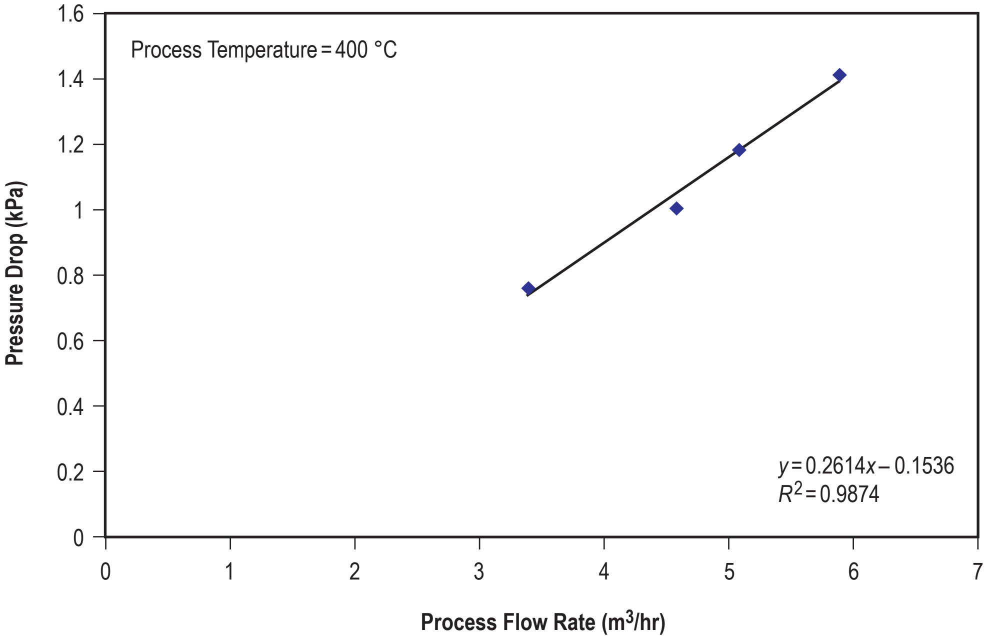

Figure 22. Effects of process flow rate on TCO assembly pressure drop.

Comparison to operational data for the TCO assembly outfitted with the fixed catalyst pellet bed results in a more modest savings. The observed pressure drop for the TCO assembly with a fixed bed of catalyst pellets is 1.1 kPa at 4.6 m^3/hr. When outfitted with the USCM reactor assembly, the pressure drop is 9 percent lower. From this comparison, it is reasonable to expect some modest pressure drop reduction for a TCO assembly that uses the USCM reactor design over a fixed bed of catalyst pellets. Further pressure drop reduction may be realized by decreasing the process airflow for niche applications and investigating a new heat exchanger assembly design.

8.4 Heater Duty Cycle

Heater duty cycle represents the percentage of time power is applied to the heater that maintains the temperature within the control deadband. Figure 23 shows heater duty cycle for 160 W power input across the range of process airflow conditions investigated. As can be expected, the heater duty increases as the process flow increases. Over the range of process flow conditions, duty cycle ranges from 75 to 100 percent.

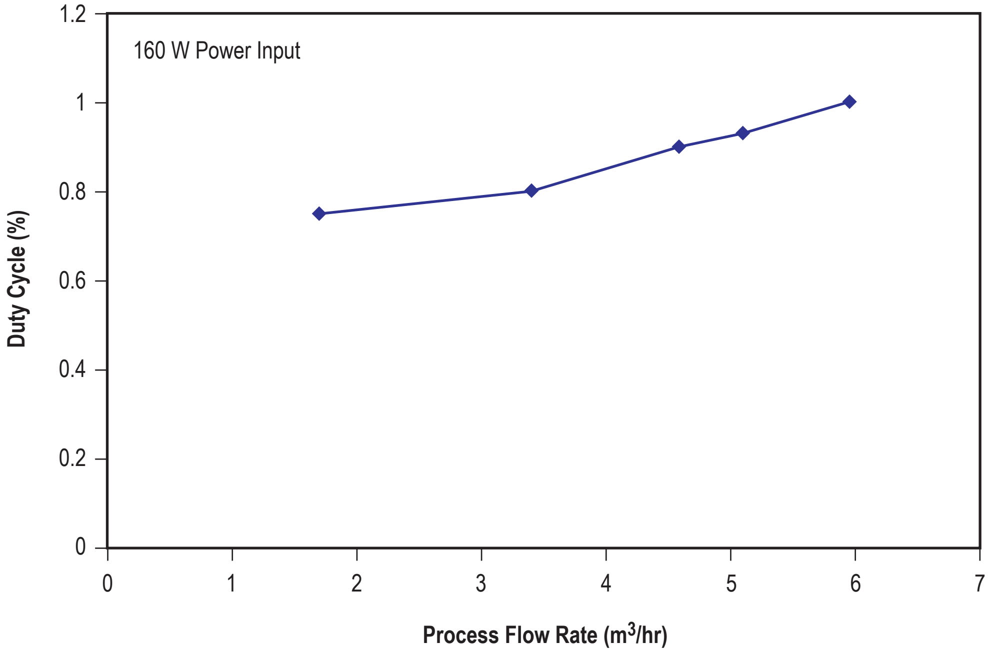

Figure 23. Duty cycle at 160 W power.

Like elapsed time for complete startup, heater duty is highly influenced by energy losses, making the TCO assembly thermal mass and external insulation important. The same TCO outfitted with a bed of catalyst pellets and immersion heater assembly typically required nearly 100 percent heater duty at 4.6-m^3/hr process airflow. By comparison, the duty cycle for the TCO outfitted with the USCM reactor assembly required 90 percent heater duty for the same flow condition. This is greater than the 72 percent duty for the TCO assembly used on board the *ISS*. As previously noted, the experimental TCO assembly possesses significantly different thermal mass and insulation characteristics compared to the unit on board the *ISS*. Because the experimental TCO outfitted with a USCM reactor assembly requires lower heater duty than the same unit outfitted with a bed of catalyst pellets and immersion heater assembly, it is reasonable to expect a modest reduction of the *ISS* unit's duty cycle if retrofit with a USCM reactor assembly.

8.5 Extended Duration Operation

After completing the performance testing runs, the USCM reactor was subjected to extended duration operation. This testing was designed according to similar testing conducted on the trace contaminant control TCO assembly for the *ISS*.[31–33] Beginning in March 2003, the process conditions were set to 4.6 m^3/hr and 160 W. Under these conditions, the process temperature is controlled to 400 ± 10 ºC. Operation was continuous with infrequent shutdown periods for test stand maintenance. No maintenance was conducted on the USCM reactor during performance testing runs or extended duration operation. The longest shutdown occurred in April 2003 when a test stand blower failed. A replacement blower was procured, installed, and the test restarted within 3 wk of the failure. CH_4 was injected periodically to check oxidation performance. This check was designed to determine if the catalytic activity remains stable over long operational periods.

Two years cumulative operation was completed on April 1, 2005. The USCM reactor was found to provide steady CH_4 oxidation performance averaging 97.6 percent for the 20 oxidation efficiency checks performed during the test. Table 7 shows the CH_4 oxidation performance check results. Power use and duty cycle remained steady throughout the testing with no deviation from that observed during the performance testing runs. Electrical power duty was found to increase during the cool months when the TCO assembly inlet temperature was periodically below 20 ºC. Inlet temperature between 25 and 30 ºC is considered best for power maintenance.

Table 7. CH_4 oxidation performance during endurance testing.

			CO_2 Concentration		
Date	Airflow (m^3/hr)	CH_4 Flow* (mL/min)	Inlet (ppm)	Outlet (ppm)	Oxidation Efficiency (%)
3/7/03	4.59	7.5	429	538	100
3/18/03	4.59	7.5	468	563	95
4/1/03	4.59	7.5	436	539	100
5/1/03	4.59	7.5	440	543	100
5/16/03	4.59	7.5	544	648	100
5/20/03	4.66	7.5	419	527	100
5/29/03	4.59	7.5	459	551	92
6/5/03	4.64	7.5	460	556	96
6/11/03	4.57	7.5	454	550	96
6/26/03	4.55	7.5	471	573	100
7/9/03	4.59	7.5	516	613	97
7/23/03	4.6	7.5	495	593	98
9/2/03	4.59	7.5	471	569	98
11/12/03	4.59	7.5	448	534	86
11/26/03	4.59	7.5	432	550	100
1/30/04	4.59	7.5	430	537	100
4/13/04	4.59	7.5	428	528	100
10/7/04	4.59	7.5	446	549	100
2/9/05	4.6	7.5	461	556	95
3/30/05	4.6	7.5	463	580	100

* Pure CH_4.

9. APPLICATIONS

Evaluating the performance of a TCO outfitted with a USCM reactor assembly has provided data necessary for defining process conditions that address a range of niche applications. These applications include spacecraft cabin air quality control, payload process gas decontamination, and commercial/residential indoor air quality control. Niche applications can extend to challenges in commercial aircraft cabin air quality control, homeland security, and chemical warfare.

9.1 Air Quality Control for Closed Environments

Niche applications most interesting to NASA are spacecraft cabin air quality control and payload process gas decontamination. Surveying the needs for these applications, a TCO based on the USCM reactor assembly operating at 3.4-m^3/hr process airflow and 120 W can provide broad spectrum oxidation of the most prevalent chemical contaminants encountered in NASA's crewed spacecraft cabins. These process conditions can provide 350 ºC operating temperature yielding >95 percent non-CH_4 VOCs and >30 percent CH_4 oxidation efficiencies. Lower single-pass CH_4 oxidation efficiency can be accommodated because the maximum allowable concentration in crewed space cabins is 3,800 mg/m^3. Generation sources are typically biological—humans, research animals, and microbial metabolism—and <1 percent single-pass efficiency is required to maintain the cabin concentration below the maximum allowed for a crew of six. Niche applications requiring more effective CH_4 removal will need higher process temperature and accompanying power.

Coupled with regenerable adsorbent modules, also based on the USCM substrate, a compact, efficient cabin air quality control and process gas decontamination system can be developed.[34,35] Figure 24 shows a conceptual process flow diagram for an air quality control system capable of maintaining CO_2 partial pressure and trace chemical contaminant concentration within allowable limits for crewed spacecraft. This process takes the most desirable features from the NASA and Russian air quality control systems on board the *ISS* and combines them to achieve power, mass, and volume savings. Depending on the application, preconditioning to remove particulate matter and moisture from the inlet air may be required. The conceptual design in figure 24 uses a 10-µm particulate filter and membrane-based desiccation stage to precondition the inlet air.

While the conceptual design shown in figure 24 is appropriate for missions up to 30 to 60 days duration when recovering water (H_2O) is not an absolute requirement, considering a modular approach to the basic design can extend its use to long-duration missions lasting months or years. Figure 25 shows a system that is amenable to recovering H_2O, removing trace contaminants, and removing CO_2. This conceptual design uses a modular approach that allows adsorbent module packages to be arranged in series. By using a stagewise, modular approach, the CO_2 product is high purity, making it suitable for reduction in either a Sabatier or Bosch reactor.

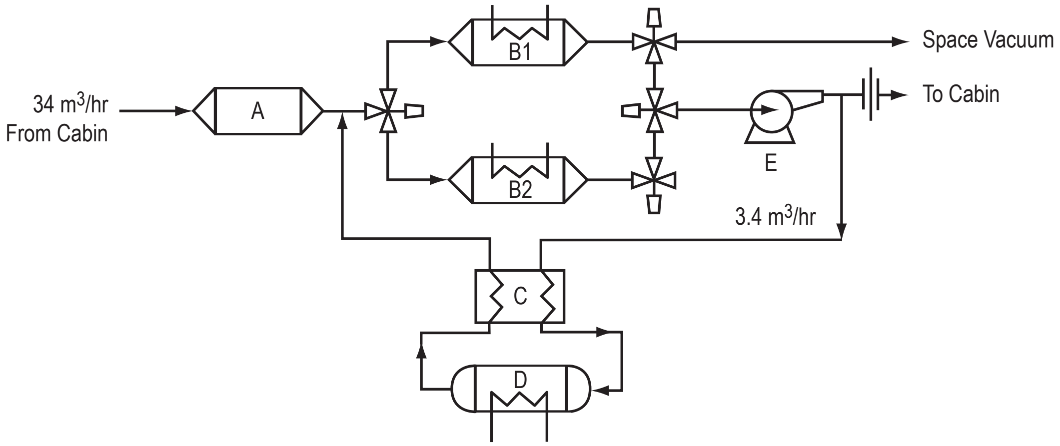

A. Expendable Guard Bed—Remove Compounds Having High Molecular Weight and Low Volatility.
B1. Regenerable Adsorbent Module 1—USCM-Based Substrate to Remove CO_2, NH_3, VOCs, and Acid Gases.
B2. Regenerable Adsorbent Module 2—USCM-Based Substrate to Remove CO_2, NH_3, VOCs, and Acid Gases.
C. Recuperative Heat Exchanger.
D. USCM Reactor Assembly—Removes CH_4, H_2, CO, Light Alcohols, and Aldehydes.
E. Blower/Air Save Pump Assembly.

Figure 24. Conceptual cabin air quality control system process design.

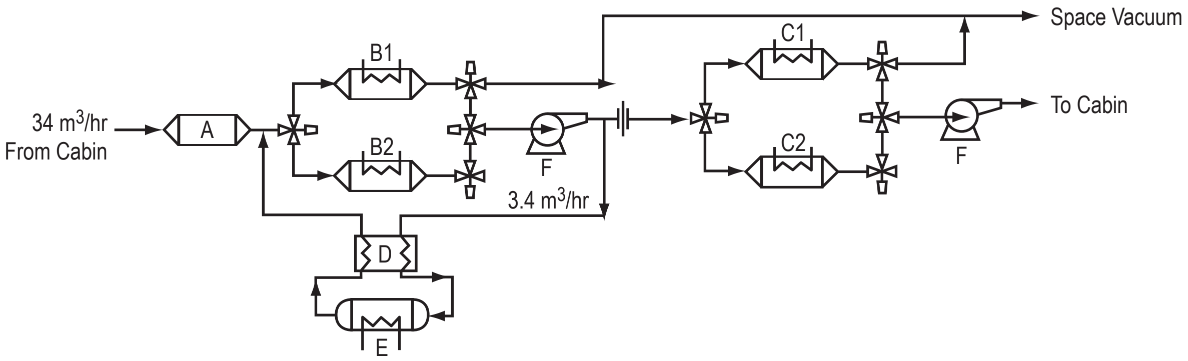

A. Expendable Guard Bed—Remove Compounds Having High Molecular Weight and Low Volatility.
B1. Regenerable Adsorbent Module 1—USCM-Based Substrate to Remove NH_3, VOCs, and Acid Gases.
B2. Regenerable Adsorbent Module 2—USCM-Based Substrate to Remove NH_3, VOCs, and Acid Gases.
C1. Regenerable CO_2 Adsorbent Module 1—USCM-Based Substrate to Remove CO_2.
C2. Regenerable CO_2 Adsorbent Module 2—USCM-Based Substrate to Remove CO_2.
D. Recuperative Heat Exchanger.
E. USCM Reactor Assembly—Removes CH_4, H_2, CO, Light Alcohols, and Aldehydes.
F. Blower/Air Save Pump Assembly.

Figure 25. Modular cabin air quality control system process design.

Smaller adsorbent modules coupled with a USCM-based TCO can be used for payload applications. Because payloads typically operate over a short time period, expendable adsorbent modules can be employed. Figure 26 shows a conceptual process design for broad spectrum control for payload process gases and working volume atmospheres. This design is based on the *ISS* contamination control equipment but directs the TCO exhaust to the inlet as recycle to eliminate the need for added postprocessing stages.

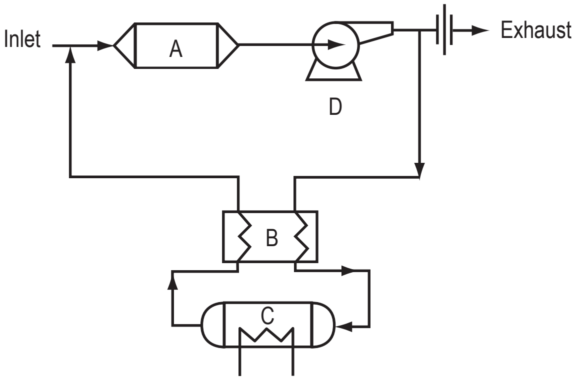

A. Expendable Guard Bed—Remove Compounds Having High Molecular Weight and Low Volatility.
B. Recuperative Heat Exchanger.
C. USCM Reactor Assembly—Removes CH_4, H_2, CO, Light Alcohols, and Aldehydes.
D. Blower/Air Save Pump Assembly.

Figure 26. Process gas cleaning system for payloads.

9.2 Commercial Aircraft

Potential exists to extend the conceptual air quality control system design to commercial aircraft. A typical ventilation rate on commercial aircraft is 34 m^3/hr/person. Assuming this rate provides up to 30 volume exchanges each hour, the approximate specific cabin volume is 1.13 m^3/person.[36] For a hypothetical airliner capable of transporting 150 people, the approximate cabin volume is 170 m^3. This volume is quite close to the *ISS* cabin volume for the U.S. segment consisting of a single laboratory module, a node, and an airlock. Total ventilation for this hypothetical airliner approaches 5,100 m^3/hr. Half of this flow, 2,550 m^3/hr, is provided by fresh, dry air from the engine bleed.

Assuming that materials of construction are similar to those used in a spacecraft, the total equipment offgassing load is similar to that experienced on board the *ISS*. In that case, fresh air makeup should be more than sufficient to control contaminants produced via equipment offgassing provided it is sufficiently clean. Contaminants from human metabolism—trace VOCs and CO_2—then become the greatest challenge.

The total human metabolic loading is 25 times that used for *ISS* design, meaning that 1,900 m^3 fresh air/hour should be sufficient to control the chief trace contaminants produced from metabolic sources. These include CO, NH_3, hydrogen (H_2), acetone, and a variety of compounds from alcohol, aldehyde, aromatic, and alkane functional classes.[37] Based on this analysis, the maximum recycle percentage for the hypothetical airliner is 63 percent to maintain trace contaminant concentration during normal flight operations.

In comparison, average CO_2 production from people is nearly 42 g/hr/person. This loading requires 3,500 m^3 fresh air/hour to control its concentration to the American Society of Heating, Refrigerating, and Air Conditioning Engineers (ASHRAE) recommended 1,800 mg/m^3 comfort threshold for 150 people.[38,39] By considering the hypothetical airliner, it is evident that CO_2 buildup is the greatest overall challenge during flight and more fresh air is necessary to keep the passengers truly comfortable. This is supported by a study of CO_2 concentration on board 44 aircraft types during 158 flights that showed air quality was the poorest during ascent and descent when ventilation recycle percentage is low.[40] Increasing the percentage of fresh air at cruising altitudes, however, has the negative impact of lowering the cabin relative humidity. This can contribute to dehydration and higher ozone concentration during extended-duration flights. While on the ground, the external contaminants become a greater challenge. Therefore, it is evident that a balance must exist between CO_2 concentration, relative humidity, ozone control, and isolation from external environmental contamination. The percentage of fresh ventilation air influences all of these air quality parameters and controlling CO_2 is the driving parameter for setting the recycle percentage. Therefore, it is necessary to understand whether using ASHRAE's recommended CO_2 comfort threshold is appropriate.

The Federal Aviation Administration's (FAA's) regulations, however, allow up to 3 percent CO_2 or 54,700 mg/m^3. Further, the FAA requires 17 m^3/hr/person ventilation—one-half the maximum ventilation rate claimed by the commercial aircraft industry.[41] Interestingly, this is 2.4 times NASA's 23,000 mg/m^3 (1.3 percent) 24-hr SMAC for CO_2 that is designed to minimize central nervous system effects, visual effects, and hyperventilation.[42] NASA's 180-day SMAC for CO_2 is 13,000 mg/m^3 (0.7 percent). While using lower cabin ventilation rates contributes to higher cabin relative humidity and lower ozone concentration, the CO_2 concentration will be >4,900 mg/m^3 for the hypothetical airliner carrying 150 passengers—2.7 times greater than ASHRAE's comfort threshold but 62 percent lower than NASA's 180-day SMAC. A study conducted for ASHRAE in 1996 recommended controlling CO_2 concentration <4,500 mg/m^3.[43] This study was conducted to support ASHRAE's effort to define standards for commercial aircraft cabin air quality. These efforts are defined in ASHRAE's SPC 161P.[44] Even to achieve 4,500 mg/m^3, a minimum 1,400 m^3 fresh air/hour must be provided to the hypothetical airliner cabin. For the FAA's minimum required ventilation rate, this represents 45 percent cabin air recycle.

From this evaluation, it is concluded that cabin air quality can be adequately maintained on board commercial airliners provided recycle does not exceed 45 percent. It is apparent that much hinges on providing a sufficient supply of fresh, clean air from the engine bleed to ensure the passengers and crew enjoy good air quality during all flight stages. While exhaust from gas turbine engines burning JP–5 aviation fuel contains significant concentrations of acetaldehyde, acrolein, benzene, HCHO, 1, 3-butadiene, propylene, toluene, and xylenes. Total VOC concentration can exceed 300 ppm.[45] Bleed air used for ventilation is apparently much cleaner. One study measured <3 ppm total VOCs in bleed air.[46] This is ≈100 times lower than the total VOC concentration found in gas turbine engine exhaust. Bleed air may contain nearly 2 ppm CO. Given these facts, the primary concern for engine bleed air quality during flight is ozone. On the ground, however, pesticides used to disinfect the cabin, VOCs from fuel fumes and engine exhaust, and other external contamination sources present the greatest threats to cabin air quality. These are transient sources that depend on the ventilation system to clean the air quickly. Therefore, USCM-based reactors can be used most effectively to oxidize ozone and provide on-demand VOC contamination control capability for transient contamination events.

9.3 Homeland Security Challenges

Beyond applications for air quality control on board spacecraft and commercial airliners, potential exists for application to commercial/residential indoor air quality control as well as a variety of homeland security challenges. Protecting buildings, aircraft, and vehicles from chemical warfare threats is an area where the USCM reactor technology can prove useful. There is striking similarity between designing to maintain air quality in a spacecraft cabin and designing to protect building and vehicle occupants from external contamination sources. Many of the chemicals of concern to protect soldiers and occupants in fixed and mobile shelters from battlefield threats are the same as for spacecraft air quality design.[47] By employing USCM reactors as part of an overall fresh air cleaning system for fixed and mobile shelters as well as homes, many homeland security issues pertaining to chemical threats can be addressed. Systems for such application can be derived from the basic design presented in figures 24–26.

10. CONCLUSIONS

The results acquired during testing of the advanced prototype USCM reactor assembly build on performance demonstration testing of the original prototype.[48] The earlier testing included exposure to random launch vibration loads. Because the advanced prototype USCM reactor and the original reactor design are nearly identical structurally, the earlier vibration testing results apply by similarity. Completing the advanced prototype testing series places the USCM reactor technology at readiness level 6 which requires successfully demonstrating prototype equipment in a relevant operational environment. The testing completed addresses all aspects of the USCM reactor operational and nonoperational environment, including thermal, humidity, random launch vibration, transportation and handling, installation, and process conditions such as process airflow, trace contaminant challenge, catalyst poisoning, and power and control interfaces. Mechanical drawings have been prepared for the niche to facilitate integration into the *ISS* air quality control system.

Results obtained from the demonstration testing series indicate that using the USCM reactor technology as a component of spacecraft cabin air quality control systems is highly feasible. Compared to thermal catalytic oxidation equipment presently used by NASA on board the *ISS,* the USCM reactor technology provides the following performance and benefits:

- CH_4 and non-CH_4 VOC oxidation comparable to the most active commercially available catalyst.

- Highly durable substrate with excellent thermal and mechanical stability.

- Rapid startup characteristics with 63 percent shorter elapsed time to oxidation reaction light-off.

- Low pressure drop with up to 38 percent estimated reduction in pressure drop.

- Improved maintainability and lower logistics mass and volume provided by a compact reactor, heater, and instrumentation package.

- Operational flexibility to tailor operational parameters to address the needs of various niche applications.

APPENDIX A—ULTRA-SHORT CHANNEL LENGTH, MONOLITHIC REACTOR ASSEMBLY INSTRUMENTATION

Reactor temperature measurement locations are shown in figure 27.

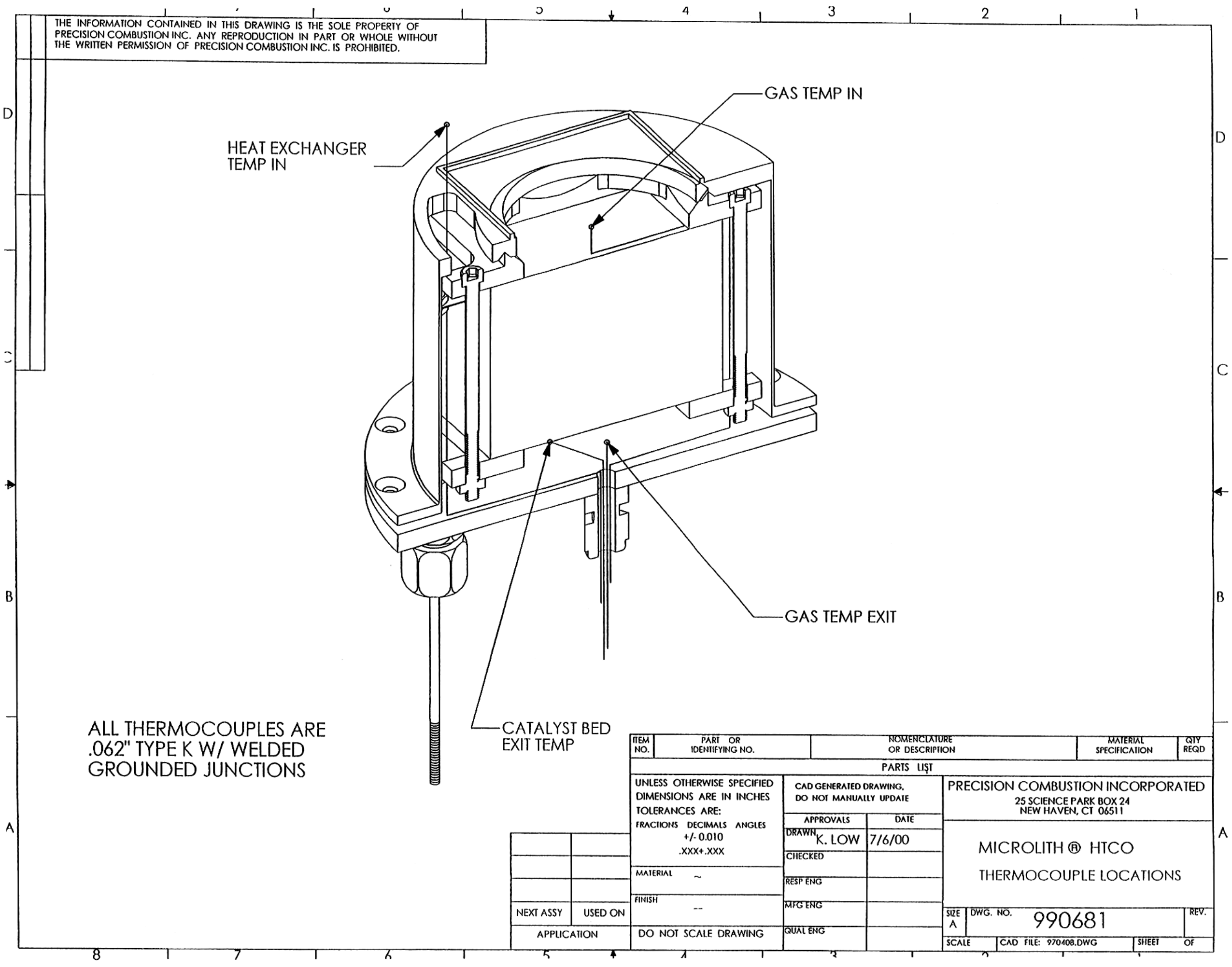

Figure 27. Reactor temperature measurement locations.

APPENDIX B—REDUCED DATA

Tables 8–13 show reduced data for oxidation efficiencies, maximum temperature, pressure drop, thermal transient duration, and power.

Table 8. Oxidation efficiencies.

Power Input (W)	Injection Rate (mL/min)	Flow Rate (cfm)	Flow Rate (m^3/hr)	CO_2 Concentration			Theory Delta (ppm)	Oxidation (decimal %)	Notes
				Inlet (ppm)	Outlet (ppm)	Delta (ppm)			
Acetone									
11	0.0171	2	3.39803763	475	470	–5	301.626275	–0.0165768	
11	0.019	2.7	4.5873508	537	537	0	248.252078	0	
44	0.014	2	3.39803763	494	498	4	246.945488	0.01619791	
44	0.019	2.7	4.5873508	494	503	9	248.252078	0.03625347	
44	0.018	3	5.09705645	500	511	11	211.667561	0.05196828	
44	0.021	3.47	5.89559529	490	492	2	213.49754	0.00936779	
96	0.014	2	3.39803763	442	452	10	246.945488	0.04049477	
96	0.019	2.7	4.5873508	499	676	177	248.252078	0.71298497	
96	0.018	3	5.09705645	584	785	201	211.667561	0.94960229	
96	0.021	3.47	5.89559529	530	714	184	213.49754	0.86183663	
160	0.014	2	3.39803763	516	790	274	246.945488	1.10955662	
160	0.018	3	5.09705645	561	878	317	211.667561	1.49763147	
160	0.021	3.47	5.89559529	511	716	205	213.49754	0.96019842	
160	0.023	2.7	4.5873508	547	553	6	300.515673	0.01996568	Outlier data
Butanol									
11	0.0212	2	3.39803763	485	480	–5	400.080505	–0.0124975	
11	0.02	2.7	4.5873508	534	537	3	279.581066	0.01073034	
44	0.015	2	3.39803763	486	518	32	283.075829	0.11304392	
44	0.022	3	5.09705645	507	555	48	276.785255	0.17341964	
44	0.026	3.47	5.89559529	490	521	31	282.803902	0.10961659	
94	0.015	2	3.39803763	513	761	248	283.075829	0.87609034	
96	0.022	3	5.09705645	592	856	264	276.785255	0.95380803	
96	0.026	3.47	5.89559529	537	820	283	282.803902	1.00069341	
160	0.015	2	3.39803763	557	882	325	283.075829	1.14810226	
160	0.02	2.7	4.5873508	488	800	312	279.581066	1.1159554	
160	0.022	3	5.09705646	551	860	309	276.785255	1.11638895	
160	0.026	3.47	5.89559529	506	815	309	282.803902	1.0926299	
44	0.02	2.7	4.5873508	516	535	19	279.581066	0.06795882	Outlier data
95	0.02	2.7	4.5873508	503	636	133	279.581066	0.47571176	Outlier data

Table 8. Oxidation efficiencies (Continued).

Power Input (W)	Injection Rate (mL/min)	Flow Rate (cfm)	Flow Rate (m^3/hr)	CO$_2$ Concentration			Theory Delta (ppm)	Oxidation (decimal %)	Notes
				Inlet (ppm)	Outlet (ppm)	Delta (ppm)			
Ethoxyethanol									
11	0.0225	2	3.39803763	468	471	3	400.964759	0.00748195	
11	0.024	2.7	4.5873508	533	533	0	316.811662	0	
44	0.018	2	3.39803763	480	583	103	320.771808	0.32110054	
44	0.024	2.7	4.5873508	492	565	73	316.811662	0.23042081	
44	0.027	3	5.09705645	492	573	81	320.771808	0.25251596	
44	0.031	3.47	5.89559529	494	532	38	318.409415	0.1193432	
94	0.019	2	3.39803763	510	845	335	338.592464	0.98939001	
96	0.027	3	5.09705646	578	907	329	320.771808	1.02565123	
96	0.031	3.47	5.89559529	537	816	279	318.409415	0.87623037	
160	0.019	2	3.39803763	537	850	313	338.592464	0.92441514	
160	0.024	2.7	4.5873508	521	834	313	316.811662	0.98796868	
160	0.027	3	5.09705645	577	933	356	320.771808	1.10982322	
160	0.031	3.47	5.89559529	512	770	258	318.409415	0.81027755	
96	0.024	2.7	4.5873508	501	598	97	316.811662	0.3061756	Outlier data
Octafluropropane									
42	5.4	2	3.39803763	469	469	0	302.415078	0	
80	5.4	2	3.39803763	558	558	0	302.415078	0	
80	7.3	2.7	4.5873508	523	523	0	302.829914	0	
80	8.1	3	5.09705645	532	532	0	302.415078	0	
80	9.3	3.47	5.89559529	508	508	0	300.187878	0	
92	5.4	2	3.39803763	506	507	1	302.415078	0.00330671	
92	7.3	2.7	4.5873508	476	476	0	302.829914	0	
120	5.4	2	3.39803763	530	544	14	302.415078	0.04629399	
120	7.3	2.7	4.5873508	502	509	7	302.829914	0.02311529	
120	8.1	3	5.09705645	533	540	7	302.415078	0.02314699	
120	9.3	3.47	5.89559529	501	503	2	300.187878	0.00666249	
160	5.4	2	3.39803763	569	585	16	302.415078	0.05290741	
160	7.3	2.7	4.5873508	553	571	18	302.829914	0.05943931	
160	8.1	3	5.09705645	517	535	18	302.415078	0.05952084	
160	9.3	3.47	5.89559529	526	534	8	300.187878	0.02664998	
Isopropanol									
11	0.024	2.7	4.5873508	496	551	55	298.877386	0.18402195	
11	0.027	3	5.09705645	507	508	1	302.613353	0.00330455	
44	0.018	2	3.39803763	490	515	25	302.613353	0.08261367	
44	0.024	2.7	4.5873508	532	532	0	298.877386	0	
44	0.027	3	5.09705645	512	522	10	302.613353	0.03304547	
44	0.031	3.47	5.89559529	495	504	9	300.384693	0.02996158	
96	0.014	2	3.39803763	515	707	192	235.365941	0.81575099	
96	0.024	2.7	4.5873508	496	720	224	298.877386	0.74947122	
96	0.027	3	5.09705645	592	804	212	302.613353	0.70056393	
96	0.031	3.47	5.89559529	529	828	299	300.384693	0.99539027	
160	0.178	2	3.39803763	507	847	340	2992.50983	0.113617	
160	0.024	2.7	4.5873508	491	651.8	160.8	298.877386	0.53801327	
160	0.027	3	5.09705645	556	854	298	302.613353	0.98475496	
160	0.031	3.47	5.89559529	509	842	333	300.384693	1.10857846	

Table 8. Oxidation efficiencies (Continued).

Power Input (W)	Injection Rate (mL/min)	Flow Rate (cfm)	Flow Rate (m^3/hr)	CO$_2$ Concentration			Theory Delta (ppm)	Oxidation (decimal %)	Notes
				Inlet (ppm)	Outlet (ppm)	Delta (ppm)			
Methane									
40	2.8	1	1.69901882	445	446	1	101.58872	0.00984361	
40	5.5	2	3.39803763	525	525	0	99.7746359	0	
90	**2.8**	**1**	**1.69901882**	**508**	**580**	**72**	**101.58872**	**0.7087401**	**Power setting incorrect**
80	**2.8**	**1**	**1.69901882**	**–**	**–**	**–**	**–**	**0.25**	**Estimated performance**
80	5.5	2	3.39803763	556	561	5	99.7746359	0.05011294	
80	7.5	2.7	4.5873508	520	521	1	100.78246	0.00992236	
80	8.3	3	5.09705645	531	531	0	100.379331	0	
80	9.6	3.47	5.89559529	508	508	0	100.375845	0	
90	2.8	1	1.69901882	443	504	61	101.58872	0.60046037	
92	5.5	2	3.39803763	505	526	21	99.7746359	0.21047433	
92	7.5	2.7	4.5873508	475	482	7	100.78246	0.06945653	
92	8.3	3	5.09705645	435	440	5	100.379331	0.04981105	
92	9.6	3.47	5.89559529	437	441	4	100.375845	0.03985022	
120	2.8	1	1.69901882	516	614	98	101.58872	0.96467403	
120	5.5	2	3.39803763	534	594	60	99.7746359	0.60135524	
120	7.5	2.7	4.5873508	503	536	33	100.78246	0.32743793	
120	8.3	3	5.09705645	535	559	24	100.379331	0.23909305	
120	9.6	3.47	5.89559529	503	521	18	100.375845	0.17932601	
160	2.8	1	1.69901882	512	614	102	101.58872	1.00404848	
160	5.5	2	3.39803763	560	656	96	99.7746359	0.96216838	
160	7.5	2.7	4.5873508	550	644	94	100.78246	0.93270198	
160	8.3	3	5.09705645	520	612	92	100.379331	0.91652335	
160	9.6	3.47	5.89559529	524	603	79	100.375845	0.78704194	
Toluene									
11	0.017	2.7	4.5873508	541	541	0	358.046045	0	
11	0.019	3	5.09705645	503	504	1	360.152198	0.0027766	
44	0.013	2	3.39803763	485	499	14	369.629887	0.03787573	
44	0.017	2.7	4.5873508	522	526	4	358.046045	0.01117175	
44	0.019	3	5.09705645	514	592	78	360.152198	0.2165751	
44	0.021	3.47	5.89559529	493	509	16	344.146647	0.04649181	
94	0.011	2	3.39803763	592	683	91	312.763751	0.29095443	
95	0.017	2.7	4.5873508	592	696	104	358.046045	0.29046543	
96	0.017	3	5.09705645	580	935	355	322.24144	1.10165843	
96	0.021	3.47	5.89559529	533	886	353	344.146647	1.02572552	
160	0.013	2	3.39803763	544	867	323	369.629887	0.87384709	
160	0.017	2.7	4.5873508	516	709	193	358.046045	0.53903682	
160	0.017	3	5.09705645	580	923	343	322.24144	1.06441927	
160	0.021	3.47	5.89559529	501	874	373	344.146647	1.08384028	

Table 9. Maximum temperature at varying power and flow conditions.

Power (W)	Flow Rate (cfm)	Temperature		Duty (%)	Upper (°F)
		Upper (°C)	Lower (°F)		
40	1	171.111111	–	100	340
80	1	290.555556	–	100	555
120	1	392.777778	–	100	739
160	1	405	596	–	761
40	2	165.555556	–	100	330
80	2	255	–	100	491
120	2	348.888889	–	100	660
160	2	405	642	–	761
40	2.7	139.888889	–	100	283
80	2.7	240.555556	–	100	465
120	2.7	330	–	100	626
160	2.7	405	663	–	761
40	3	153.333333	–	100	308
80	3	246.111111	–	100	475
120	3	318.888889	–	100	606
160	3	405	664	–	761
40	3.47	138.333333	–	100	281
80	3.47	235	–	100	455
120	3.47	321.111111	–	100	610
160	3.47	394.444444	–	100	742

Table 10. HTCO assembly pressure drop.

Power (W)	Flow Rate (cfm)	Delta *P* (kPa)	Maximum Temperature (°C)	Delta *P* (in H_2O)	Maximum Temperature (°F)	Power* (W)	Flow Rate* (cfc)
160	2	0.75719764	404.444444	3.04	760	11	3
92	2	0.6675295	293.333333	2.68	560	11	2
42	2	0.46577618	172.222222	1.87	342	11	2.7
11	2	0.37112647	71.6666667	1.49	161	40	3.47
160	2.7	1.00129425	404.444444	4.02	760	44	3
95	2.7	0.89169985	294.444444	3.58	562	44	2.7
44	2.7	0.69243732	163.333333	2.78	326	42	2
11	2.7	0.54299041	72.1666667	2.18	161.9	96	3.47
160	3	1.18063053	404.444444	4.74	760	96	3
96	3	1.01374816	293.222222	4.07	559.8	92	2
44	3	0.76466999	160.777778	3.07	321.4	95	2.7
11	3	0.65258481	70.1666667	2.62	158.3	160	2
160	3.47	1.40729167	404.444444	5.65	760	160	2.7
96	3.47	1.11836099	279.833333	4.49	535.7	160	3
40	3.47	0.88920907	154	3.57	309.2	160	3.47

* Sort by maximum temperature.

Table 11. Composite oxidation efficiency.

Power Input (W)	Injection Rate (mL/min)	Flow Rate (cfm)	CO_2 Concentration			Theory Delta (ppm)	Oxidation (decimal %)		Average Air Temperature	
			Inlet (ppm)	Outlet (ppm)	Delta (ppm)				(°C)	(°F)
160	0.014	2	516	790	274	246.945488	1.10955662	1	387.78	730
160	0.019	2	537	850	313	338.592464	0.92441514	0.92441514	385.28	725.5
160	0.178	2	507	847	340	2992.50983	0.113617	0.113617	385.06	725.1
160	0.013	2	544	867	323	369.629887	0.87384709	0.87384709	385.06	725.1
160	0.015	2	557	882	325	283.075829	1.14810226	1	383.39	722.1
96	0.014	2	515	707	192	235.365941	0.81575099	0.81575099	309	588.2
96	0.014	2	442	452	10	246.945488	0.04049477	0.03649635	293.33	560
94	0.015	2	513	761	248	283.075829	0.87609034	0.76307692	320.57	609.03
94	0.019	2	510	845	335	338.592464	0.98939001	0.98939001	319.56	607.2
94	0.011	2	592	683	91	312.763751	0.29095443	0.29095443	319.06	606.3
44	0.018	2	490	515	25	302.613353	0.08261367	0.08261367	179.06	354.3
44	0.018	2	480	583	103	320.771808	0.32110054	0.32110054	175.11	347.2
44	0.013	2	485	499	14	369.629887	0.03787573	0.03787573	173.17	343.7
44	0.015	2	486	518	32	283.075829	0.11304392	0.09846154	172.56	342.6
44	0.014	2	494	498	4	246.945488	0.01619791	0.01459854	172.22	342
11	0.0212	2	485	480	–5	400.080505	–0.0124975	0	72.83	163.09
11	0.0171	2	475	470	–5	301.626275	–0.0165768	0	70	158
11	0.0225	2	468	471	3	400.964759	0.00748195	0.00748195	63.67	146.6
160	0.023	2.7	547	553	6	300.515673	0.01996568	1	396.11	745
160	0.017	2.7	516	709	193	358.046045	0.53903682	0.53903682	395.72	744.3
160	0.024	2.7	521	834	313	316.811662	0.98796868	0.98796868	394.72	742.5
160	0.024	2.7	491	651.8	160.8	298.877386	0.53801327	0.53801327	393.11	739.6
160	0.02	2.7	488	800	312	279.581066	1.1159554	1	391.61	736.9
96	0.019	2.7	499	676	177	248.252078	0.71298497	0.71298497	294.44	562
96	0.024	2.7	501	598	97	316.811662	0.3061756	0.3061756	291.5	556.7
96	0.024	2.7	496	720	224	298.877386	0.74947122	0.74947122	287.33	549.2
95	0.017	2.7	592	696	104	358.046045	0.29046543	0.2046543	395.72	744.3
95	0.02	2.7	503	636	133	279.581066	0.47571176	0.42628205	291.17	556.1
44	0.024	2.7	492	565	73	316.811662	0.23042081	0.23042081	165.28	329.5
44	0.019	2.7	494	503	9	248.252078	0.03625347	0.03625347	163.33	326
44	0.02	2.7	516	535	19	279.581066	0.06795882	0.06089744	161.83	323.3
44	0.024	2.7	532	532	0	298.877386	0	0	161.68	323.03
44	0.017	2.7	522	526	4	358.046045	0.01117175	0.01117175	161.22	322.2
11	0.024	2.7	533	533	0	316.811662	0	0	72.81	163.05
11	0.019	2.7	537	537	0	248.252078	0	0	72.22	162
11	0.02	2.7	534	537	3	279.581066	0.01073034	0.00961538	72.22	161.99
11	0.024	2.7	496	551	55	298.877386	0.18402195	0.18402195	70.72	159.3
11	0.017	2.7	541	541	0	358.046045	0	0	68.91	156.04
160	0.018	3	561	878	317	211.667561	1.49763147	1	396.11	745
160	0.022	3	551	860	309	276.785255	1.11638895	1	396	744.8
160	0.017	3	580	923	343	322.24144	1.06441927	0.96619718	395.53	743.96
160	0.027	3	556	854	298	302.613353	0.98475496	0.98475496	395.11	743.2
160	0.027	3	577	933	356	320.771808	1.10982322	1	373.34	704.01
96	0.027	3	578	907	329	320.771808	1.02565123	0.9241573	297.06	566.7
96	0.022	3	592	856	264	276.785255	0.95380803	0.85436893	294.11	561.4

Table 11. Composite oxidation efficiency (Continued).

Power Input (W)	Injection Rate (mL/min)	Flow Rate (cfm)	CO$_2$ Concentration			Theory Delta (ppm)	Oxidation (decimal %)		Average Air Temperature	
			Inlet (ppm)	Outlet (ppm)	Delta (ppm)				(°C)	(°F)
96	0.018	3	584	785	201	211.667561	0.94960229	0.6340694	293.22	559.8
96	0.027	3	592	804	212	302.613353	0.70056393	0.70056393	289.89	553.8
96	0.017	3	580	935	355	322.24144	1.10165843	1	281.39	538.5
44	0.019	3	514	592	78	360.152198	0.2165751	0.19659007	164.17	327.5
44	0.027	3	512	522	10	302.613353	0.03304547	0.03304547	163.5	326.3
44	0.022	3	507	555	48	276.785255	0.17341964	0.15533981	162.89	325.2
44	0.018	3	500	511	11	211.667561	0.05196828	0.03470032	160.78	321.4
44	0.027	3	492	573	81	320.771808	0.25251596	0.22752809	158.11	316.6
11	0.019	3	503	504	1	360.152198	0.0027766	0.00252039	70.17	158.3
11	0.027	3	507	508	1	302.613353	0.00330455	0.00330455	69.72	157.5
160	0.021	3.47	501	874	373	344.146647	1.08384028	1	400.78	753.4
160	0.021	3.47	511	716	205	213.49754	0.96019842	0.96019842	400.17	752.3
160	0.026	3.47	506	815	309	282.803902	1.0926299	1	398.67	749.6
160	0.031	3.47	512	770	258	318.409415	0.81027755	0.81027755	397.22	746.99
160	0.031	3.47	509	842	333	300.384693	1.10857846	1	396.78	746.2
96	0.031	3.47	529	828	299	300.384693	0.99539027	0.8978979	291.28	556.3
96	0.021	3.47	533	886	353	344.146647	1.02572552	0.9463807	290.28	554.5
96	0.026	3.47	537	820	283	282.803902	1.00069341	0.91585761	286.39	547.5
96	0.021	3.47	530	714	184	213.49754	0.86183663	0.86183663	279.83	535.7
96	0.031	3.47	537	816	279	318.409415	0.87623037	0.87623037	273.11	523.6
44	0.026	3.47	490	521	31	282.803902	0.10961659	0.10032362	154.33	309.8
44	0.021	3.47	490	492	2	213.49754	0.00936779	0.00936779	154	309.2
44	0.031	3.47	495	504	9	300.384693	0.02996158	0.02702703	151	303.8
44	0.031	3.47	494	532	38	318.409415	0.1193432	0.1193432	149.11	300.4
44	0.021	3.47	493	509	16	344.146647	0.04649181	0.04289544	146.94	296.5

Table 12. Thermal transient duration.

Power (W)	Flow Rate		Time		
	(cfm)	(m^3/hr)	To 300 °F (hr)	To 500 °F (hr)	To 760 °F (hr)
40	1	1.699019	2.483	–	–
80	1	1.699019	0.34	2.533	–
120	1	1.699019	0.0633	0.783	–
160	1	1.699019	0.0283	0.25	1.5
40	2	3.398038	–	–	–
80	2	3.398038	0.65	–	–
120	2	3.398038	0.217	1.233	–
160	2	3.398038	0.0667	0.55	2.517
40	2.7	4.587351	–	–	–
80	2.7	4.587351	0.767	–	–
120	2.7	4.587351	0.283	1.5	–
160	2.7	4.587351	0.1	0.633	3.567
40	3	5.097056	4.333	–	–
80	3	5.097056	0.683	–	–
120	3	5.097056	0.333	1.633	–
160	3	5.097056	0.117	0.683	4.233
40	3.47	5.895595	–	–	–
80	3.47	5.895595	0.8	–	–
120	3.47	5.895595	0.322	1.6	–
160	3.47	5.895595	0.118	0.717	–

Table 13. Power duty.

Power (W)	Flow Rate		Duty Cycle		
	(cfm)	(m^3/hr)	On (min)	Off (min)	Decimal Percent
160	1	1.699019	4	1	0.75
160	2	3.398038	5	1	0.8
160	2.7	4.587351	10	1	0.9
160	3	5.097056	14	1	0.93
160	3.5	5.946566	–	–	1

REFERENCES

1. Carter, R.N.; Bianchi, J.F.; Pfefferle, W.C.; et al.: "Unique Metal Monolith Catalytic Reactor for Destruction of Airborne Trace Contaminants," SAE 972432, Society of Automotive Engineers, Warrendale, PA, pp. 1–2, July 1997.

2. Roychoudhury, S.; Muench, G.; Bianchi, J.F.; et al.: "Development and Performance of Microlith^{TM} Light-Off Preconverters for LEV/ULEV," SAE 971023, Society of Automotive Engineers, Warrendale, PA, pp. 56–57, February 1997.

3. Carter, R.N.; Bianchi, J.F.; Pfefferle, W.C.; et al.: "Unique Metal Monolith Catalytic Reactor for Destruction of Airborne Trace Contaminants," SAE 972432, Society of Automotive Engineers, Warrendale, PA, p. 3, July 1997.

4. Perry, J.L.: "Elements of Spacecraft Cabin Air Quality Control Design," *NASA/TP—1998–207978*, NASA Marshall Space Flight Center, MSFC, AL, pp. 36–48, May 1998.

5. Perry, J.L.; Curtis, R.E.; Alexandre, K.L.; et al.: "Performance Testing of a Trace Contaminant Control Subassembly for the *International Space Station*," SAE 981621, Society of Automotive Engineers, Warrendale, PA, pp. 1–2, July 1998.

6. Mitchell, K.L.; Bagdigian, R.M.; Carrasquillo, R.L.; et al.: "Technical Assessment of *Mir*-1 Life Support Hardware for the *International Space Station*," *NASA TM–108441*, NASA Marshall Space Flight Center, MSFC, AL, pp. 39–52, March 1994.

7. Curtis, R.E.; Perry, J.L.; and Abramov, L.H.: "Performance Testing of a Russian *Mir* Space Station Trace Contaminant Control Assembly," SAE 972267, Society of Automotive Engineers, Warrendale, PA, pp. 1–2, July 1997.

8. Graf, J.; Wright, J.; and Bahr, J.: "A Regenerable Sorbent Bed for Trace Contaminant Removal," SAE 1999–01–2071, Society of Automotive Engineers, Warrendale, PA, pp. 4–7, July 1999.

9. Buoni, C.M.; Arthur, M.F.; Balog, P.P.; et al.: "Space Station Contamination in Pressurized Environments: Issues and Options," NAS10–11033, Battelle Columbus Laboratories, Columbus, OH, Sec. 4, pp. 15–18, April 12, 1985.

10. Carter, R.N.; Bianchi, J.F.; Pfefferle, W.C.; et al.: "Unique Metal Monolith Catalytic Reactor for Destruction of Airborne Trace Contaminants," SAE 972432, Society of Automotive Engineers, Warrendale, PA, pp. 3–6, July 1997.

11. Perry, J.L.; and Humphries, W.R.: "Process Material Management in the Space Station Environment," SAE 880996, Society of Automotive Engineers, Warrendale, PA, pp. 1–4, July 1988.

12. Silverberg, P.M.: "Stocking the Explorer's Craft: Technologies Developed for Space Travel Have Earthly Application in the CPI," *Chemical Engineering,* Vol. 97, p. 45, August 2001.

13. Hines, A.L.; Ghosh, T.K.; Loyalka, S.K.; and Warder, R.C.: *Indoor Air Quality and Control*, Prentice Hall, NJ, pp. 20–65, 1993.

14. Perry, J.; and Graf, J.: "Spacecraft Cabin Air Quality Control and Its Application to Tight Buildings," AIAA–95–1050, American Institute of Aeronautics and Astronautics, Washington, DC, p. 7, April 1995.

15. Molhave, L.: "Volatile Organic Compounds and the Sick Building Syndrome," *Environmental Toxicants,* M. Lippmann (ed.), Van Nostrand Reinhold, NY, pp. 643–644, 1992.

16. Block, S.S.: "Microorganisms, Sick Buildings, and Building Related Illnesses," *Disinfection, Sterilization, and Preservation,* S. Block (ed.), Lea & Febiger, Philadelphia, PA, p. 1111, 1991.

17. Graf, R.: "Bleed Air Quality Test of the Pratt & Whitney Aircraft JT8D-209 Turbofan Engine," PWA–5624, United Technologies Pratt & Whitney Aircraft Group, East Hartford, CT, pp. 7–8, February 15, 1979.

18. "Toxic Organic Contaminants in the Exhaust of Gas Turbine Engines," AESO 12-90, Aircraft Environmental Support Office Naval Aviation Depot, San Diego, CA, pp. 3–4, September 1990.

19. Olcott, T.; Lamparter, R.; Maine, B.; et al.: "Design, Fabrication, and Test of a Trace Contaminant Control System," LMSC–D462467, Lockheed Missiles and Space Co., Inc., Sunnyvale, CA, pp. 54–60, 143–187, November 28, 1975.

20. Evans, T.: "Design, Fabrication, and Test of a Developmental Metal Monolith Catalytic Converter for Trace Contaminant Control," Final Progress Report Under Contract NAS8–40369–5152, ION Corporation, Huntsville, AL, With Contractor Precision Combustion, Inc., North Haven, CT, pp. 13–15, App. A, August 31, 2000.

21. Leban, M.I.; Kawasaki, E.H.; and Conine, G.P.: "Performance Characterization of Activated Carbon and Oxidation Catalyst for Gaseous Trace Contaminant Control," SAE 911548, 21st International Conference on Environmental Systems, Society of Automotive Engineers, pp. 1–2, Warrendale, PA, 1991.

22. Wright, J.D.; Chen, B.; and Wang, C.M.: "Trace Contaminant Oxidation Catalyst Poisoning Investigation," NAS8–38250–15, TDA Research, Inc., Wheat Ridge, CO, pp. 16–20, March 22, 1996.

23. Ibid, pp. 21–46.

24. Ibid, pp. 24–30.

25. Amman, K.: “Development of the Catalytic Oxidizer Technology for the European Space Programme,” SAE 891533, 19th Intersociety Conference on Environmental Systems, Society of Automotive Engineers, Warrendale, PA, p. 7, 1989.

26. Perry, J.L.: “Octafluoropropane Concentration Dynamics On Board the *International Space Station*, SAE 2003–01–2651, 33rd International Conference on Environmental Systems, Society of Automotive Engineers, Warrendale, PA, pp. 2–3, 2003.

27. Young, J.: “PCI Reactor Evaluation for FEANICS,” FEANICS–RPT–0–130, NASA Glenn Research Center, Cleveland, OH, pp. 7–8, March 17, 2005.

28. Pfefferle, W.; Roychoudhury, S.; and Bianchi, J.: “Unique Metal Monolith Catalytic Converter for Small Efficient Trace Contaminant Control System,” NAS8–40132, Precision Combustion, Inc., North Haven, CT, pp. 16–17, July 26, 1994.

29. Armstrong, M.D.: “Space Station Environmental Control and Life Support System Test Data and Summary Report for the MSFC Refurbished Trace Contaminant Control Subsystem,” ECLSS/TECH/EL92–002, NASA Marshall Space Flight Center, MSFC, AL, p. 8, February 28, 1992.

30. Olcott, T.; Lamparter, R.; Maine, B.; et al.: “Design, Fabrication, and Test of a Trace Contaminant Control System,” LMSC–D462467, Lockheed Missiles and Space Company, Inc., Sunnyvale, CA, pp. 98–101, November 28, 1975.

31. Perry, J.L.: “Trace Contaminant Control Subassembly High Temperature Catalytic Oxidizer Life Testing Requirements,” NASA Memorandum ED62(51–92), NASA Marshall Space Flight Center, MSFC, AL, pp. 6–8, May 5, 1992.

32. Perry, J.L.: “Revised Environmental Control and Life Support Life Test Requirements,” NASA Memorandum ED62(107–92), NASA Marshall Space Flight Center, MSFC, AL, pp. 1–2, November 17, 1992.

33. Tatara, J.D.; and Perry, J.L.: “International Space Station *Alpha* Trace Contaminant Control Subassembly Life Test Final Report,” *NASA TM–108488*, NASA Marshall Space Flight Center, MSFC, AL, pp. 1–3, March 1995.

34. Roychoudhury, S.; Walsh, D.; and Perry, J.: “Microlith Based Sorber for Removal of Environmental Contaminants, SAE 2004–01–2442, 34th International Conference on Environmental Systems, Society of Automotive Engineers, Warrendale, PA, pp. 1–3, 2004.

35. Mulloth, L.M.; Perry, J.L.; and LeVan, M.D.: “Integrated System Design for Air Revitalization in Next Generation Crewed Spacecraft,” SAE 2004–01–2373, 34th International Conference on Environmental Systems, Society of Automotive Engineers, Warrendale, PA, pp. 2–3, 2004.

36. Hunt, E.H.; and Space, D.R.: “The Airplane Cabin Environment—Issues Pertaining to Flight Attendant Comfort,” The Boeing Company, Seattle, WA, p. 1, Undated.

37. Perry, J.L.: “Elements of Spacecraft Cabin Air Quality Control Design,” *NASA/TP—1998–207978*, NASA Marshall Space Flight Center, MSFC, AL, pp. 27–30, May 1998.

38. Wieland, P.O.: “Designing for Human Presence in Space—An Introduction to Environmental Control and Life Support Systems,” *NASA RP–1324*, NASA Marshall Space Flight Center, MSFC, AL, p. 6, 1994.

39. “Ventilation for Acceptable Indoor Air Quality,” ASHRAE STD 62–2001 and Addenda, American Society of Heating, Refrigerating, and Air Conditioning Engineers, 2001.

40. “Breathing on a Jet Plane—How Fresh is the Air?,” *Consumer Reports*, pp. 501–506, August 1994.

41. “Report on Commercial Aircraft Cabin Air Quality Control Techniques and Proposed Air Quality Standards,” Holcomb Environmental Services, Inc., Olivet, MI, p. 5, November 18, 1996.

42. James, J.T.: “Spacecraft Maximum Allowable Concentrations for Airborne Contaminants,” JSC 20584, NASA Johnson Space Center, Houston, TX, p. 3, June 1999.

43. “Report on Commercial Aircraft Cabin Air Quality Control Techniques and Proposed Air Quality Standards,” Holcomb Environmental Services, Inc., Olivet, MI, p. 35, November 18, 1996.

44. “Air Quality Within Commercial Aircraft,” ASHRAE SPC 161P, American Society of Heating, Refrigerating, and Air Conditioning Engineers, Public Review Draft, Undated.

45. “Toxic Organic Contaminants in the Exhaust of Gas Turbine Engines,” AESO Report No. 12–90, Aircraft Environmental Support Office, Naval Aviation Depot, San Diego, CA, pp. 7–8, September 1990.

46. Graf, R.: “Bleed Air Quality Test of the Pratt and Whitney Aircraft JT8D-209 Turbofan Engine, PWA–5624, United Technologies Pratt and Whitney Aircraft Group, East Hartford, CT, pp. 3–4, February 15, 1979.

47. Perry, J.L.; and LeVan, M.D.: “Air Purification in Closed Environments—Overview of Spacecraft Systems,” COLPRO 02, NBC Defense Collective Protection Conference, Orlando, FL, p. 9, October 2002.

48. Perry, J.L.; Frederick, K.R.; Carter, R.N.; and Tatara, J.D.: “Performance Demonstration of a Metal Monolith Catalytic Converter for Trace Contaminant Control,” *NASA/TM—1999–209262*, NASA Marshall Space Flight Center, MSFC, AL, pp. 23–40, April 1999.

REPORT DOCUMENTATION PAGE

Form Approved
OMB No. 0704-0188

1. AGENCY USE ONLY *(Leave Blank)*

2. REPORT DATE
September 2005

3. REPORT TYPE AND DATES COVERED
Technical Memorandum

4. TITLE AND SUBTITLE
Thermal Catalytic Oxidation of Airborne Contaminants by a Reactor Using Ultra-Short Channel Length, Monolithic Catalyst Substrates
(MSFC Center Director's Discretionary Fund Final Report, Project No. 02–18)

5. FUNDING NUMBERS

6. AUTHORS
J.L. Perry, K.M. Tomes, and J.D. Tatara*

7. PERFORMING ORGANIZATION NAME(S) AND ADDRESS(ES)
George C. Marshall Space Flight Center
Marshall Space Flight Center, AL 35812

8. PERFORMING ORGANIZATION REPORT NUMBER
M–1145

9. SPONSORING/MONITORING AGENCY NAME(S) AND ADDRESS(ES)
National Aeronautics and Space Administration
Washington, DC 20546–0001

10. SPONSORING/MONITORING AGENCY REPORT NUMBER
NASA/TM—2005–214061

11. SUPPLEMENTARY NOTES
Prepared by the Spacecraft and Vehicle Systems Department, Engineering Directorate
*Qualis Corporation, 6767 Old Madison Pike, Suite 105, Huntsville, AL 35806

12a. DISTRIBUTION/AVAILABILITY STATEMENT
Unclassified-Unlimited
Subject Category 54
Availability: NASA CASI 301–621–0390

12b. DISTRIBUTION CODE

13. ABSTRACT *(Maximum 200 words)*

Contaminated air, whether in a crewed spacecraft cabin or terrestrial work and living spaces, is a pervasive problem affecting human health, performance, and well being. The need for highly effective, economical air quality processes spans a wide range of terrestrial and space flight applications. Typically, air quality control processes rely on absorption-based processes. Most industrial packed-bed adsorption processes use activated carbon. Once saturated, the carbon is either dumped or regenerated. In either case, the dumped carbon and concentrated waste streams constitute a hazardous waste that must be handled safely while minimizing environmental impact. Thermal catalytic oxidation processes designed to address waste handling issues are moving to the forefront of cleaner air quality control and process gas decontamination processes. Careful consideration in designing the catalyst substrate and reactor can lead to more complete contaminant destruction and poisoning resistance. Maintenance improvements leading to reduced waste handling and process downtime can also be realized. Performance of a prototype thermal catalytic reaction based on ultra-short waste channel, monolith catalyst substrate design, under a variety of process flow and contaminant loading conditions, is discussed.

14. SUBJECT TERMS
air quality, life support, contamination control, catalytic oxidation, volatile organic compounds, catalyst, reactor, environmental control

15. NUMBER OF PAGES
64

16. PRICE CODE

17. SECURITY CLASSIFICATION OF REPORT	**18. SECURITY CLASSIFICATION OF THIS PAGE**	**19. SECURITY CLASSIFICATION OF ABSTRACT**	**20. LIMITATION OF ABSTRACT**
Unclassified	Unclassified	Unclassified	Unlimited

NSN 7540-01-280-5500

Standard Form 298 (Rev. 2-89)
Prescribed by ANSI Std. 239-18
298-102

National Aeronautics and
Space Administration
IS04
George C. Marshall Space Flight Center
Marshall Space Flight Center, Alabama
35812